**Article:**
Soltan, R and Mountney, NP (2016) Interpreting complex fluvial channel and barform architecture: Carboniferous Central Pennine Province, northern England. Sedimentology, 63 (1). 207 - 252. ISSN 0037-0746

https://doi.org/10.1111/sed.12224

Received Date : 28-Oct-2014

Revised Date : 14-Jun-2015

Accepted Date : 04-Aug-2015

Article type : Original Manuscript

# Interpreting complex fluvial channel and barform architecture: Carboniferous Central Pennine Province, northern England

Roman Soltan[1] and Nigel P. Mountney[1]

1 – Fluvial Research Group, School of Earth and Environment, University of Leeds, Leeds, LS2 9JT, UK
*(E-mail: ee07r2s@leeds.ac.uk)*

**Associate Editor – Charlie Bristow**

## Short Title – Interpreting channel and barform architecture

## ABSTRACT

The Bashkirian Lower Brimham Grit of North Yorkshire, England, is a fluvio-deltaic sandstone succession that crops out as a complex series of pinnacles, the three-dimensional arrangement of which allows high-resolution architectural analysis of genetically-related lithofacies assemblages. Combined analysis of sedimentary graphic log profiles, architectural panels and palaeocurrent data have enabled three-dimensional geometrical relationships to be established for a suite of architectural elements so as to develop a comprehensive depositional model. Small-scale observations of facies have been related to larger-scale architectural elements to facilitate interpretation of the palaeoenvironment of deposition to a level of detail that has rarely been attempted previously, thereby allowing interpretation of formative processes. Detailed architectural panels form the basis of a semi-quantitative technique for recording the variety and complexity of the sedimentary lithofacies present, their association within recognizable architectural elements and, thus, the inferred spatio-temporal relationship of neighbouring elements. Fluvial channel-fill elements bounded by erosional surfaces are characterized internally by a hierarchy of sets and cosets with subtly varying compositions, textures and structures. Simple, cross-bedded sets represent in-channel migration of isolated mesoforms (dunes); cosets of both trough and planar-tabular cross-bedded facies represent lateral-accreting and downstream-accreting macroforms (bars) characterized by highly variable, yet predictable, patterns of palaeocurrent indicators.

This is an Accepted Article that has been peer-reviewed and approved for publication in the *Sedimentology*, but has yet to undergo copy-editing and proof correction. Please cite this article as an "Accepted Article"; doi: 10.1111/sed.12224

Relationships between sandstone-dominated strata bounded by third-order and fifth-order surfaces, which represent in-channel bar deposits and incised channel bases respectively, chronicle the origin of the preserved succession in response to autocyclic barform development and abandonment, major episodes of incision probably influenced by episodic tectonic subsidence, differential tilting and fluvial incision associated with slip on the nearby North Craven Fault system. Overall, the succession represents the preserved product of an upper-delta plain system that was traversed by a migratory fluvial braid-belt system comprising a poorly-confined network of fluvial channels developed between major sandy barforms that evolved via combined lateral-accretion and downstream-accretion.

**Keywords:** Architectural element analysis, braided fluvial system, depositional palaeoenvironment, facies analysis, Lower (First) Brimham Grit, upper-delta plain.

## INTRODUCTION

The relationship between the internal lithofacies composition and the external geometrical form of architectural elements that comprise fluvial successions in general, and those representative of upper-delta plain settings in particular, has been discussed previously by numerous workers (e.g. Miall, 1985; Olsen *et al*., 1995; Ghazi & Mountney, 2009). However, criteria with which to distinguish between the preserved successions of channelized upper-delta plain systems and alluvial plain systems in the sedimentary record are subjective and recognition of fluvial successions that occur specifically in upper-delta plain settings is not straightforward (Fielding, 1985). An important step in establishing robust criteria for the recognition of the specific architectural form of preserved fluvio-deltaic sedimentary successions is the requirement to collect sufficient data such that the detailed palaeoenvironmental significance of three-dimensional lithofacies, architectural-element and bounding-surface arrangements can be determined (Alexander, 1989; Miall, 2014). Development of such detailed palaeoenvironmental depositional models is typically constrained by the extent and three-dimensional nature of the available outcrop; the lack of opportunity to examine the detailed internal facies architecture and bounding surface arrangements associated with architectural elements representative of channels, sheets, barforms and superimposed dunes is a common limiting problem. Although there have previously been numerous studies related to the fluvial and deltaic sedimentology of the Carboniferous Central Pennine Province, UK (e.g. McCabe, 1977; Bristow, 1988; Collinson, 1988; Gawthorpe *et al*., 1989; Martinsen *et al*., 1995; Hallsworth & Chisholm, 2008; Waters *et al.,* 2008), few have hitherto sought to interpret channel and barform architecture at a bed by bed scale and relate the collated data to formative processes through examination of preserved three-dimensional architectural relationships (Fig. 1).

The present study seeks to gain insight into the sedimentology of upper-delta plain successions through a detailed examination of the sedimentary architecture of the Carboniferous (Bashkirian) Lower Brimham Grit succession exposed at Brimham Rocks, North Yorkshire, England. The study area represents a well-exposed example of a fluvial upper-delta plain succession (cf. Bristow, 1988;

Fraser & Gawthorpe, 2003; Wilson, 2006). The outcrop takes the form of a series of tors, each separated by gullies formed where exposed joint surfaces have been subject to weathering processes (Linton, 1955; Palmer & Radley, 1961). Crucially, the tors and their bounding gullies are arranged in a variety of orientations such that the detailed 3D sedimentary architecture can be interpreted to a level of detail that typically is not possible with most outcropping successions. Thus, the Brimham Grit affords a rare opportunity to interpret the internal architecture of a fluvial upper-delta plain succession in unprecedented detail.

The aim of this article is to document and interpret channel and barform architecture through detailed field-based examinations of Bashkirian (Namurian) successions formed in a fluvial channel system that traversed a proximal delta plain in an overall low-accommodation setting, relative to more distal parts of the system that accumulated in a relatively high-accommodation setting. Specific objectives of this study are as follows: (i) to develop a depositional model explaining how sediment distribution patterns and mechanisms influenced sediment accumulation; (ii) to demonstrate and interpret the sedimentological significance of relationships between neighbouring architectural elements and their associated facies components in terms of processes responsible for the generation of fluvial channels and barforms; (iii) to establish a depositional palaeoenvironment highlighting sediment provenance and palaeocurrent regimes responsible for generating the preserved 3D stratigraphic architecture; and (iv) to consider the relative roles of autogenic and allogenic processes in governing sediment delivery mechanisms.

This research is important, timely, novel and of broad appeal for the following reasons: (i) it demonstrates how quantitative facies relationships and depositional models can be constructed that can potentially be applied as analogues for other similar systems; (ii) it utilizes an exceptionally well-exposed suite of outcrops to further current understanding of three-dimensional channel and barform architecture within an ancient upper-delta plain succession; (iii) it demonstrates relationships between small-scale facies components and larger-scale architectural elements; (iv) it demonstrates the three-dimensional geometries of elements and their relationships to neighbouring elements, thereby facilitating detailed palaeoenvironmental interpretations; and (v) it demonstrates the relationships and palaeoenvironmental significance of various fluvial architectural elements from outcrops that have not previously been examined in detail.

## GEOLOGICAL SETTING

The type section for the Lower Brimham Grit is Brimham Rocks, a series of moorland tors that crop out over an area of 2 $km^2$ north of the village of Summerbridge, North Yorkshire, UK (Fig. 2). The Lower Brimham Grit (Bashkirian) is a pebbly sandstone succession that forms part of the Hebden Formation of the Carboniferous Millstone Grit Group (Fig. 3A and C; Jones, 1943; Wilson & Thompson, 1965; Waters, 2011a; Waters *et al.*, 2011b).

Carboniferous rocks underlie *ca* 75% of northern England (Stone *et al.,* 2010) and sedimentation in the Central Pennine Province (Fig. 4A) occurred in a variety of terrestrial, deltaic, paralic and marine depositional environments (Gilligan, 1919; Guion *et al.*, 2010; Stone *et al.*, 2010). From the Serpukhovian to the mid-Bashkirian (*ca* 330 to 318 Ma) sedimentation was generally associated with the evolution of fluvial, deltaic or deep-water clastic depositional environments (Guion *et al.,* 2010) and infilling of the Stainmore Basin (Fig. 4A and B) facilitated the subsequent southerly migration of fluvio-deltaic systems across the older Askrigg Block (Martinsen, 1990, 1993). The presence of such large deltaic systems with a northerly provenance has long been inferred in the Craven Basin (Fig. 4A and B) of North Yorkshire (Gilligan, 1919) and their preserved remnants are represented by Namurian Millstone Grit strata within the region (Walker, 1966; Martinsen, 1990).

Sedimentary successions within the Craven Basin are all of Carboniferous age or younger (Gawthorpe, 1987). Cyclic episodes of delta progradation and subsequent flooding during the Namurian are thought to have spanned *ca* 180 to 185 kyr and have been attributed to glacio-eustatic mechanisms (Martinsen, 1993; Martinsen *et al*., 1995). Such episodes generated extensive mudstone units that represent the various marine bands that occur intercalated with distributary channel and mouth-bar deposits related to highstand systems tracts and incised valley fills (e.g. Corfield *et al.,* 1996). During the mid-Serpukhovian (latest Pendleian *ca* 327.5 Ma), the basin accumulated clastic turbidites and initial Millstone Grit sediments were deposited (Martinsen, 1990). These deposits were subsequently overlain by coarse-grained sandstone bodies representative of major fluvio-deltaic plains. Within the study area, such remnants infer the presence of an upper-delta plain, exposed as a variety of large-scale channel sandbodies and their component lithofacies.

*Tectonic setting*

The intracratonic Craven sedimentary basin (Arthurton, 1984; Martinsen *et al.,* 1995) forms a major north-east to south-west trending half-graben (Fraser & Gawthorpe, 2003) and represents one of a series of linked rift-related basins that make up the Dinantian rift province – also known as the Central Pennine Province – present across much of northern and central England (Fig. 4A; Arthurton, 1983). The Carboniferous palaeobathymetry of the intracratonic Central Pennine Province (Elliott, 1989; Martinsen, 1990) was dictated by north–south extensional tectonics arising from the northward extension of the Variscan (Hercynian) Front (Gawthorpe *et al.,* 1989; Fraser & Gawthorpe, 1990; Martinsen, 1990, 1993). Numerous carbonate platforms and detached deep-water basins developed between fault blocks and a distinctly segregated 'block and basin' bathymetry developed (Collinson *et al.,* 1990). Basin architecture was governed mainly by fault propagation, growth and cessation (Gawthorpe & Leeder, 2000); "burial or breaching of crossover basement ridges" facilitated the evolution of hydrologically closed rifts into open rift systems with though-going sediment transport pathways (Gawthorpe & Leeder, 2000). Such activity probably generated a pathway for sediment distribution into the eastern part of the Craven Basin via a relay fault zone situated between the northern (south-west to north-east trending) and southern (west/south-west to east/north-east trending) extensions of the North Craven Fault System (Fig. 4B and C; cf. Reid, 1996; Gobo *et al.*, 2014). This relay zone may have also contributed to the development of the Harrogate Basin (Cooper & Burgess, 1993) which Martinsen (1990) considered

to be the eastern extension of the Craven Basin.

Although extensional stresses are thought to have dominated during the Dinantian and early Serpukhovian, subsequent basin development was governed primarily by post-extensional thermal sag (Leeder, 1982, 1988; Gawthorpe *et al.,* 1989; Martinsen *et al.,* 1995; Fraser & Gawthorpe, 2003). During this period, the Carboniferous succession on the Askrigg Block was not affected by Variscan tectonic activity (Arthurton *et al.,* 1988) and a distinct bathymetric relief between the Askrigg Block and Craven Basin became established (Collinson, 1988) such that the 'block and basin' bathymetric style became dominated by shallow-water and deep-water sedimentation, respectively (Cooper & Burgess, 1993). Tectonic activity along the North Craven Fault may have led to lateral tilting that influenced the course of the fluvial system responsible for the deposition of the Lower Brimham Grit.

*Kinderscoutian palaeogeography*

During the Serpukhovian to mid-Bashkirian (Pendleian to Alportian *ca* 330 to 322 Ma), accumulation and progradation of the sedimentary succession between the Askrigg Block and Craven Basin is initially attributed to turbidite-fronted delta sedimentation influenced by a distinct shelf-edge boundary (Martinsen, 1990, 1993; Martinsen *et al.,* 1995). As the rate of subsidence waned in the Craven Basin and progradation of the deltaic system continued, bathymetric disparities diminished and a southerly-dipping ramp and shallow-water delta system evolved (Martinsen, 1990, 1993; Martinsen *et al.,* 1995). Although deltaic systems are commonly classified on the basis of fluvial-dominance, wave-dominance or tide-dominance (Galloway, 1975), they are generally regressive systems (Elliott, 1989) influenced by many additional controls that govern temporal and spatial evolution (see Miall, 1976; Bridge, 2003; Bhattacharya, 2006, 2010).

Waters & Condon (2012) relate Bashkirian sedimentation (*ca* 322.8 to 314.6 Ma) within the broader region to glacial influence related to the Gondwanan Late Palaeozoic Ice Age. These authors argue for a protracted interglacial period (*ca* 321.5 to 319.5 Ma) that was associated with an episode of subdued eustatic sea-level oscillations, during which the appearance of *Reticuloceras* forms a valuable sequential biostratigraphic marker. Sedimentation within much of the Central Pennine Province was characterized by the gradual accumulation of hemipelagic and distal turbidite sediments linked to a relatively stable and high sea-level and no significant fluvial incision (Waters & Condon, 2012). The latter part of this period is represented by the N7 mesothem (Ramsbottom, 1977), the Kinderscoutian *Reticuloceras eoreticulatum* ($R_{1b}$) ammonoid zone and the *Reticuloceras nodosum* goniatite zone ($R_{1b}2$) (*ca* 320.2 to 319.5 Ma; Waters & Condon, 2012). Although work by Ramsbottom (1977) argues that deposition of the Lower Brimham Grit occurred within this episode, subsequent work places the Lower Brimham Grit and equivalent Lower Plompton Grit of the Harrogate area (Reid, 1996 and Dale, 2011, respectively) above the *Reticuloceras reticulatum* ($R_{1c}1$) ammonoid zone, which forms the base of the N8 mesothem (*ca* 319.5 Ma; Waters & Condon, 2012; Fig. 3B). Work by Dale (2011) also implies that the Lower Plompton Grit does not extend above the *Reticuloceras coreticulatum* ($R_{1c}4$) ammonoid zone (*ca* 319.25 Ma; Waters & Condon, 2012; Fig. 3B), which constrains the duration of the Lower Brimham Grit to less than 250 kyr (i.e. between the $R_{1c}1$ and $R_{1c}4$ ammonoid zones). This episode coincided with the onset of latest Namurian to earliest

Westphalian glaciation that induced near-basinwide progradation of coarse, pebbly and generally sheet-like fluvio-deltaic sandbodies in the Pennine Basin (Waters & Condon, 2012). Thus, deposition of the Lower Brimham Grit succession was probably influenced by both stable, high and falling eustatic sea-level associated with the transition from an interglacial to glacial period, respectively.

*Brimham Grit*

Phillips (1836) was the first author to introduce the term 'Brimham Grits' to the geological literature. The term was applied as a group name encompassing Carboniferous strata above the Lower Follifoot Grit (Fig. 3C), which included the widespread occurrence of a coarse-grained feldspathic sandstone succession located at Brimham Rocks (Thompson, 1957). The only detailed accounts of the succession are those in the doctoral theses of Thompson (1957), Wilson (1957) and Reid (1996). Composed largely of coarse-grained quarzto-felspathic sandstone, the Lower Brimham Grit is present continuously throughout the eastern margin of the Craven Basin, ranging in preserved thickness from *ca* 9 to 122 m (Thompson, 1957). Locally, the succession is *ca* 50 m thick within the Brimham Rocks study area.

Work by Walker (1952) and Thompson (1957) demonstrates that the Lower Brimham Grit south of Pateley Bridge is underlain by an angular unconformity. Possible explanations for the origin of this unconformity are as follows: (i) variable rates of accommodation generation between the footwall and outer regions of the hangingwall; (ii) tectonically influenced syn-sedimentary deformation and erosion; (iii) fluvial incision influenced by base-level; and (iv) non-deposition arising from a switching of the main sediment delivery pathway. Thus, the stratigraphic signature of the Lower Brimham Grit succession conceivably records a combination of both autogenic and allogenic influences. Reid (1996) interpreted the unconformity at the base of the Lower Brimham Grit to have been associated with significant erosion and attributed its development to accumulation of part of an 'alluvial delta-front grit sequence' that later became overlain by an erosional 'major channel grit sequence', which subsequently evolved upwards into an 'alluvial flood plain sequence' representative of the progradation of the delta plain.

The Lower Brimham Grit is overlain by the Brimham Shale, a marine interval that divides the Lower and Upper Brimham Grit successions (Fig. 3C) and records a minor transgression. The overlying Upper Brimham Grit is also a coarse-grained feldspathic sandstone and is somewhat similar to the Lower Brimham Grit (Thompson, 1957; Reid, 1996). Ramsbottom (1979), Martinsen (1993) and Martinsen *et al.* (1995) noted that clastic sediments comprising the Brimham Grits were derived principally from systems that flowed over the Askrigg Block and the eastern margin of the Craven Basin (Fraser & Gawthorpe, 2003) from a northerly provenance (i.e. Laurentia and Baltica). Consisting of predominantly eroded remnants of Scottish and Norwegian Caledonian Mountains, these clastic sediments were transported within a palaeo-drainage basin that probably extended *ca* 450 km and *ca* 950 km in length towards the north and north-east, respectively, and included the Harrogate and Cleveland basins (Martinsen, 1990). During latter stages of the Namurian (late

Arnsbergain to late Chokieran), sedimentation from a westerly provenance developed a more significant role (Martinsen, 1990; Fraser & Gawthorpe, 2003) and the Wales-Brabant High (Fig. 4A) also contributed to the influx of sediment into the main Craven Basin from a southerly direction (Hallsworth *et al.*, 2000; Hallsworth & Chisholm, 2008). These varied sediment routing directions are a potential cause of varied palaeocurrents observed in successions in the north and north-west of the basins, including those at Brimham Rocks. The extent of the drainage basin is comparable with that of the medium-scale (*ca* 700 km long) Wisconsin sand-bed braided river that drains an area of *ca* 31,000 $km^2$ (Mumpy *et al.*, 2007).

## DATA AND METHODS

The complex array and three-dimensional nature of the outcropping gritstone tors exposed at Brimham Rocks (Figs 1 and 2) generate features suited to high-resolution architectural analysis. These features enable detailed examination and interpretation of architectural elements and their internal lithofacies compositions in orientations parallel and perpendicular to the inferred palaeocurrent, both laterally and vertically. Thirteen 1D measured graphic logs, 2D architectural panels that collectively portray *ca* 320 $m^2$ of the exposed stratigraphic succession, two pseudo-3D box panels, and 485 palaeocurrent readings measured from foreset, set, coset and channel bounding surfaces (expressed as arrows depicting mean palaeocurrent azimuth-dips) were collated from the Lower Brimham Grit succession at Brimham Rocks. Data were collated to establish the detailed depositional palaeoenvironment responsible for generating the preserved stratigraphic architecture. Graphic logs and architectural panels record the variety of sedimentary lithofacies present, their association to one another, their delineation into sets and cosets defined by bounding surfaces and the arrangement of such sets into larger-scale architectural elements. Although the three-dimensional nature of the exposed succession is ideal for comparison of outcrop versus modern fluvial architecture (for example, derived from GPR data: Best *et al.*, 2003; Skelly, *et al.*, 2003; Mumpy *et al.*, 2007; Ashworth *et al.*, 2011), detailed consideration of such comparisons is beyond the scope of this study.

Palaeocurrent data – a key requirement for constraining fluvial facies models (Bridge, 1985) – have been grouped according to lithofacies type in which they occur and relationship to parent architectural elements. The majority of palaeocurrent data were measured from foreset azimuth-dips, trough axes and channel bounding surface dips and these are delineated from those readings that relate to the attitude of erosional bounding surfaces. From the combined lithofacies, bounding-surface, architectural-element and palaeocurrent data, pseudo-3D box panels have been constructed to determine how the individual lithofacies are arranged into common associations defining a variety of architectural elements. These associations include single-storey, multilateral and multi-storey channel sandbodies, downstream-accreting and laterally-accreting bar elements, interdune elements and sheet-like gravel sandbodies. Differentiation of elements and their style of juxtaposition has been undertaken principally via the lateral tracing of erosional bounding surfaces using the techniques of Miall (1985, 2010a, 2010b, 2014). This differentiation has facilitated the establishment of facies models that account for the origin of the preserved succession in response to

a range of processes (cf. Collinson, 1996). Such analysis has involved the construction of a detailed depositional model that relates small-scale observations of facies to larger-scale architectural elements, thereby enabling the interpretation of the depositional palaeoenvironment within a representative part of a major delta-plain system.

## SEDIMENTOLOGY AND STRATIGRAPHY

### *Lithofacies*

Lithofacies associated with outcrops observed at Brimham Rocks have been classified into 14 commonly occurring and distinctive sub-facies (Figs 5 and 6; Table 1). The majority of the observed lithofacies are composed of quartzo-feldspathic (subarkose) grains that range in modal grain size from medium sand to granules, with small to medium pebbles variably comprising >15% of the deposits. Collectively the lithofacies display characteristics typical of largely channelized fluvial deposits, forming facies associations typical of sedimentation in channel bar, dune, interdune and channel settings (Figs 6, 7 and 8; Table 1; cf. Bristow, 1993; Collinson, 1996; Reesink & Bridge, 2007, 2009; Miall, 2010a, 2010b, 2014; Colombera *et al.*, 2012a, 2012b; 2013). Representative sedimentary graphic log profiles (Fig. 9) obtained from two main locations (Figs 2C and 7; Locations 1 and 2) record the vertical facies arrangement typical of the preserved Lower Brimham Grit. Due to the complexity of the outcrops, descriptions and interpretations of the characteristic lithofacies recognized at Brimham Rocks are representative and not exhaustive. References made below to the scale of cross-bedded sets, the shape of troughs and dune elements, for example, are typical values for the features observed in outcrops of the Brimham Grit but variations from these typical styles are common. The 14 identified sub-facies form the basic components of two fluvial facies associations that are characteristic of barform and in-channel deposition, respectively.

### *Architectural elements*

Six representative architectural elements are recognized (Fig. 10) and each has been allocated an element code based on the schemes of Miall (2010a, 2010b, 2014) and Colombera *et al.* (2012a, 2012b, 2013): channels (CH), sandy bedforms (SB), downstream-accretion macroform type 1 (DA1), downstream-accretion (or oblique) macroform type 2 (DA2), lateral-accretion macroform (LA) and interdune mesoform or macroform (ID). Identification and interpretation of observed bounding surfaces are founded on the Miall (2010b) classification of bounding surfaces. Although vertical aggradation and lateral accretion are both associated with the growth of the majority of sandstone elements (Miall, 2010b), descriptions and interpretations of the characteristic architectural elements recognized at Brimham Rocks are representative and not exhaustive (cf. Allen, 1983; Bridge, 1985; Bristow, 1996). Hence, in a manner similar to that of the study of Cain (2009) and Cain & Mountney (2009), the lithofacies and architectural elements presented in this study are unique to Brimham Rocks and are constructed exclusively from the observations and interpretations made within the study area. Within the following interpretations, approximate palaeocurrent velocities have been estimated with reference to grain size and critical erosion velocity analysis conducted by Sundborg (1956). The following equation has been used to infer approximate original mean dune height (cf.

Leclair & Bridge, 2001; Leclair, 2011):

$$h_m = 2.9(\pm 0.7)s_m \quad (1)$$

where $h_m$ and $s_m$ represent mean dune height and mean cross-set thickness, respectively. Mean grain sizes associated with architectural elements vary from medium sand to granules, with granules being the modal grain size in some elements. Hence, the grain size component suggests that the minimum palaeocurrent velocity was in the region of *ca* 0.6 m $s^{-1}$ (Sundborg, 1956). Reesink & Bridge (2007, 2009) note that a decrease in flow stage and related bed shear stress is likely to result in a decrease in bedload grain size. Given this, the widespread occurrence of alternating foresets of relatively fine and coarse-grained strata is probably related to low-flow and high-flow stages, respectively (Reesink & Bridge, 2007, 2009). Hence, flood events should act to locally and temporarily increase bedload grain size. Although the three-dimensional nature of the studied outcrops yields exceptional detail with regard to internal lithofacies associations, the lateral extent of elements examined remains relatively poorly constrained because many of the larger elements exceed the extent of the outcrop; dimensions of these elements are therefore either partial or unlimited (*sensu* Geehan & Underwood, 1993).

**Channel bar and channel fill architectural elements**

*Downstream-accretion macroform (DA1)*

*Description:* Component lithofacies of this element are fine-grained sandstone to granulestone with ≤10% small pebble content that is represented predominantly by small-scale trough cross-bedding [for example, *Stsx <1.5 m*; Figs 5, 9 (log profiles F to N and P) and 10; Table 1]. Primary sedimentary structures consist of low-angle-inclined to high-angle-inclined foresets that form <1.5 m wide and <0.2 m thick trough cross-bedded sets that overlap both vertically and laterally to form compound cosets. Compound cosets of strata form sandbodies up to 2.0 m thick, 30.0 m wide and 50.0 m in lateral extent. Element bounding surfaces are generated by first-order set and second-order coset boundaries. Packages of several sets are bounded by second-order surfaces that exhibit horizontal or sub-horizontal, sharp and commonly erosional contacts with underlying packages. Sharp, sub-horizontal to low-angle-inclined set contacts also exhibit evidence of erosion with underlying sets. Foresets are inclined at angles of up to 25˚, whereas set and coset bounding surfaces are typically inclined at angles of up to 20˚ and 10˚, respectively. Although surfaces associated with foresets, sets and cosets vary in their respective dip inclinations, they each exhibit comparable mean azimuths to the south (Fig. 10).

*Interpretation:* The internal arrangement of lithofacies within examples of this element records the southerly migration of relatively small (<1.5 m wide) sinuous-crested dunes (3D mesoforms). Preserved set thicknesses of <0.2 m suggest that the original mean dune height was in the region of

0.4 to 0.7 m (Leclair, 2011). Such dunes developed along the crest or front of a migrating channel bar that itself represents a macroform responsible for generating a coset of strata (Allen, 1982; Miall, 2010b; cf. Ashworth *et al.*, 2011). The arrangement of lithofacies indicates down-current-dipping set and coset bounding surfaces generated through limited sediment input into a relatively shallow channel subjected to turbulent flow conditions that resulted in dune migration and climb at positive but subcritical angles (Collinson *et al.*, 2006). This interpretation is analogous to that of Bristow (1993) who inferred downstream-accretion of bedforms during high-flow stage in the Brahmaputra River, Bangladesh, and to Bristow (1988) who documented similar bedforms forming in very shallow braided rivers associated with the deposition of the Namurian Rough Rock Group within the Pennine Basin, northern England. Similarly, Ghinassi (2011) associates large-scale inclined beds with migrating channel bars that are related to braided fluvial sediments observed in Holocene river deposits, Tuscany, Italy. Reesink & Bridge (2009) relate dune-formed cosets to large-scale low-angle sets that are generated by down-climbing dunes. Stacked sets separated by first-order set boundaries indicate repeated bedform migration probably as a train of dunes over a larger bar surface (Miall, 2010b; cf. Ashworth *et al.*, 2011). More steeply inclined first-order surfaces denote reactivation surfaces (Collinson, 1970). Minor erosion associated with these surfaces records episodes of minor bedform adjustment (Miall, 2010b) associated with fluctuations in bedform alignment due to changed flow direction (cf. Haszeldine, 1983). Second-order coset bounding surfaces record the downstream migration of larger bars over which the smaller dunes migrated. The erosion associated with these surfaces implies either bar readjustment due to a variation in palaeocurrent direction or localized scour in front of advancing barforms (Miall, 2010b). These interpretations are comparable to those of Reesink *et al.* (2014) who infer that the initial phases of bar development within the Río Paraná, Argentina, are influenced by the downstream migration and amalgamation of unit (singular) bars. Reesink *et al.* (2014) also note that bars within multi-channel rivers are dominated by dune sets. The similar azimuths for both inclined foresets and first-order and second-order bounding surfaces demonstrate that both the smaller-scale dunes and the larger-scale bars migrated in a downstream direction (Miall, 2010b, 2014). For examples where the range of azimuths is more varied, dune-scale bedforms may have migrated obliquely over, around and down curved bar-form fronts.

*Downstream and oblique-accretion macroform (DA2)*

*Description:* Component lithofacies of this element are coarse-grained to very-coarse-grained sandstone and granulestone with 5 to 10% small pebble content that are represented from bottom to top by a distinctive vertical succession of facies [Figs 5, 9 (log profile E) and 10; Table 1]. Lowermost facies in the element consist of small-scale trough cross-bedding (*Stsx <1.5 m*) characterized by westerly dipping, low-angle-inclined (≤10˚) foresets and <1.50 m wide, <0.20 m thick, easterly dipping (≤13˚), cross-cutting trough cross-bedded sets. Packages of several sets are bounded by second-order surfaces that exhibit sharp, sub-horizontal (≤12˚), easterly dipping and commonly erosional overlying contacts, and sharp, sub-horizontal (≤12˚) easterly dipping erosional fifth-order underlying channel base surfaces that delimit the base of the element. Overlying facies of very large-scale planar cross-bedding (*Sl-hpx >2.0 m*) are characterized by low-angle-inclined to moderate-angle-inclined (≤20˚) planar cross-bedded sets. Internally, sets contain *ca* 0.02 m thick foreset laminae that exhibit distinct normal grading with each lamina fining-up from granulestone to

coarse sandstone. Additionally, sets may be characterized by south-westerly or westerly-dipping first-order reactivation surfaces. Individual sets of this facies are up to 3 m thick and are bounded at their base by sharp, low-angle-inclined (≤10˚), sub-horizontal, erosional second-order bounding surfaces, whereas top surfaces are commonly irregular, erosional, second-order contacts. The uppermost facies in examples of this element is medium-scale trough cross-bedding (*Stmx 1.5 to 3.0 m*), which is characterized by primary sedimentary structures consisting of predominantly low-angled-inclined foresets that form *ca* 1.0 m thick and 1.5 to 3.0 m wide, cross-cutting trough cross-bedded sets. Sets of this facies are bounded at their base by an irregular erosional second-order contact. Trends from palaeocurrent data indicate that, although the foresets and reactivation surfaces possess a general south-westerly trending azimuth, set, coset and channel bounding surfaces generally have dips that possess easterly dipping azimuths (Fig. 10). Examples of this element form sandbodies up to 5.0 m thick, >4.0 m wide and >4.0 m long (lateral dimensions poorly constrained due to limited outcrop extent).

*Interpretation:* The internal arrangement of lithofacies within examples of this element records climbing trough cross-bedded sets that are indicative of a generally westerly migration of small-scale sinuous-crested dunes. These sandbodies accumulated in a channel-floor setting, with the base of the channel itself forming a fifth-order bounding surface (the base of the element). This interpretation is similar to features described by Bristow (1993) who envisaged downstream-accreting bedforms that developed during high-flow stage in the Brahmaputra River, Bangladesh, and also to bedforms known to form in very shallow braided rivers associated with the deposition of the Namurian Rough Rock Group within the Pennine Basin (Bristow, 1988). Similarly, Ghinassi *et al.* (2009) attribute small-scale trough and planar cross-bedding (3D and 2D mesoforms, respectively) from fluvial sediments of the Alat Formation (Pleistocene Dandiero Basin, Eritrea) to shallow low sinuosity channel deposits. Additionally, Reesink *et al.* (2014) demonstrate that dune sets make up the thalweg deposits observed in the Río Paraná, Argentina, and Ashworth *et al.* (2011) show that dunes in the South Saskatchewan River, Canada, increase in size towards the channel thalweg. Preserved set thicknesses of <0.2 m suggest that the original mean dune height was 0.4 to 0.7 m (Leclair, 2011), which implies that limited sediment input into a relatively shallow channel within which flow conditions resulted in dune migration and climb at (net) subcritical angles (Collinson *et al.*, 2006). The second-order overlying bounding surfaces in the middle part of examples of this element and associated change in lithofacies denote a change in flow conditions (Miall, 2010b). Overlying westerly migrating planar-tabular low-angle to medium-angle-inclined very large-scale cross-bedding (Fig. 10) are most obviously interpreted as an alternate bar (3D macroform; McCabe, 1977; Collinson, 1996; Collinson *et al.*, 2006; Miall, 2010b). The relative increase in bedform size implies an increase in palaeo-discharge, which probably facilitated the processes that gave rise to the distinct normal grading in the foresets of these deposits. Repeated grainflow avalanche deposits record alternating pulses of finer-grained and coarser-grained sediments passing over bar crestlines, associated with the accumulation of coarse sediments within leeside scours of migrating asymmetrical bedforms with lee slopes characterized by relatively finer sediments (see Smith, 1972; Reesink & Bridge, 2007, 2009). For other successions of Kinderscoutian age present in the Central Pennine Province, McCabe (1977) interpreted alternate bars that were considered to have formed within distributary channels between 1.0 to 2.0 km wide and 30.0 to 40.0 m deep. Similarly, the scale of the forms observed here suggests that these alternate bars were likely to have formed in

relatively deep channels (cf. Reesink & Bridge, 2009; Ashworth *et al.*, 2011; Reesink *et al.*, 2014). The shallow inclined (≤12˚) first-order, second-order and fifth-order bounding surface dips of this element also correspond with the observation by McCabe (1977) of distributary channel dips being in the region of ≤10˚ and that of Bristow (1993) that bed bounding surfaces, with very low depositional dips, correspond to channels possessing high width to depth ratios. Bar heights may vary between half and bankfull depth (cf. Bristow, 1987; Bridge, 2003; Reesink *et al.*, 2014). Hence, the preserved planar cross-bedded bar thickness (*ca* 3.0 m) suggests that the depth of the host channel was in the region of 3.0 to 6.0 m (cf. Bristow, 1987; Bridge, 2003; Reesink *et al.*, 2014). Relative to the underlying unit, this implies an increase in channel depth and sediment input under laminar flow conditions. Alternate bar forms may have been attached to and have migrated obliquely to a channel bank (McCabe, 1977; Collinson, 1996; Collinson *et al.*, 2006); alternatively they may develop as large mid-channel forms (Collinson, 1996; Collinson *et al.*, 2006) or may develop as they migrate into a scour pool associated with a channel confluence (McCabe, 1977; Collinson, 1996; Collinson *et al.*, 2006). Furthermore, Reesink *et al.* (2014) describe comparable facies to that of facies *Sl-hpx >2.0 m* (this study), which are associated with barforms (Facies 1A of Reesink *et al.*, 2014, their figure 6B, E and F and table 2). For example, bar *U2* of Reesink *et al.* [2014, their figures 2B and 7A (B1 to B5) and table 1] initially developed obliquely as a bank attached elongated bar and subsequently became a detached and reworked channel bar (cf. Ashworth *et al.*, 2011), probably facilitated through chute channel activity (cf. Brierley, 1991; Ghinassi, 2011). Such observations are consistent with the formation of a bank attached alternate bar (see above). First-order reactivation surfaces within the alternate bar record relatively minor localized erosion, associated with one or more of the following: fluctuations in palaeocurrent direction (Miall, 2010b); oscillations in flow stage (Collinson, 1970) facilitated by flood events (Ashworth *et al.*, 2011); variations in bedform alignment (Haszeldine, 1983); slip-face reworking (Collinson, 1996) by superimposed bedforms (Reesink & Bridge, 2007, 2009; Ashworth *et al.*, 2011). The uppermost deposits in these elements record the passage and accumulation of medium-scale sinuous-crested dunes whose presence implies a turbulent flow regime associated with shallower water and the overall infilling of a channel (cf. McCabe, 1977).

*Channel (CH)*

*Description:* Component lithofacies of this element are a coarse-grained to very coarse-grained sandstone to granulestone with 5 to 10% small pebble content that are represented from bottom to top by a variable vertical succession of facies [Figs 5, 9 (log profiles E and G to Q) and 10; Table 1]. Lowermost facies in the element consist of small-scale trough cross-bedding (*Stsx <1.5 m*) characterized by westerly dipping, low-angle-inclined (≤10˚) foresets and <1.50 m wide and <0.20 m thick easterly dipping (≤13˚), cross-cutting trough cross-bedded sets. Packages of several sets of this facies are bounded at their base by a sharp, sub-horizontal (≤12˚), easterly dipping, fifth-order erosional surface that defines the base of the channel element. At their top, packages are delimited by second-order surfaces that exhibit sharp, sub-horizontal (≤12˚), easterly dipping and commonly erosional overlying contacts. Overlying facies of very-large-scale planar cross-bedding (*Sl-hpx >2.0 m*) are characterized by low-angle to moderate-angle-inclined (≤20˚) planar cross-bedded sets. Internally, sets contain *ca* 0.02 m thick foreset laminae that exhibit distinct normal grading with each lamina fining-up from granulestone to coarse-grained sandstone. Many sets are additionally

characterized by south-westerly-dipping or westerly-dipping first-order reactivation surfaces. Individual sets of this facies may be up to 3 m thick and are bounded at their base by sharp, low-angle-inclined (≤10˚), sub-horizontal, erosional second-order bounding surfaces, whereas top surfaces are commonly irregular, erosional, second-order contacts. The overlying facies in examples of this element is medium-scale trough cross-bedding (*Stmx 1.5 to 3.0 m*), which is characterized by low-angle-inclined foresets that form *ca* 1.0 m thick and 1.5 to 3.0 m wide, cross-cutting trough cross-bedded sets bounded at their base by an irregular erosional second-order contact. Trends from palaeocurrent data indicate that foresets possess generally southerly and south-westerly trending azimuths; by contrast, set, coset and channel bounding surfaces generally have dips that possess easterly trending azimuths (Fig. 10). Lithofacies assemblages that characterise this element may form sandbodies up to 5.0 m thick, >70.0 m wide and >30.0 m long. Such channel elements may possess an erosional basal contact with underlying planar laminated facies (*Spl/b)* characterized by a fine-grained to medium-grained sandstone that is notably lacking in mica and which is characterized by small-scale 2 to 4 mm thick southerly dipping sub-horizontal (≤8˚) planar laminations. The laminations commonly form 10 to 30 mm thick bed sets with sharp, southerly dipping, sub-horizontal (≤10˚), erosional second-order contacts between component bed sets and easterly dipping, sub-horizontal (≤12˚), erosional fifth-order surface contact between the uppermost bed set and overlying channel element.

*Interpretation:* The internal arrangement of lithofacies within examples of this element records climbing trough cross-bedded sets that are indicative of a generally westerly migration of small-scale sinuous-crested dunes. These sandbodies accumulated in a channel-floor setting that itself formed a fifth-order bounding surface (the base of the element; see also architectural element DA2 above). Preserved set thicknesses of <0.2 m suggest that the original mean dune height was 0.4 to 0.7 m (Leclair, 2011), which implies limited sediment input into a relatively shallow channel within which turbulent flow conditions resulted in dune migration and climb at (net) subcritical angles (Collinson *et al.*, 2006). The second-order overlying bounding surfaces in the middle part of the element and associated change in lithofacies denote a change in flow conditions (Miall, 2010b). Overlying westerly migrating planar-tabular low-angle to medium-angle-inclined very large-scale cross-bedded sets (Fig. 10) are best interpreted as alternate bar deposits (McCabe, 1977; Collinson, 1996; Collinson *et al.*, 2006; Miall, 2010b; see architectural element DA2 above). The scale of the bedforms observed here suggests that these alternate bars were likely to have formed within deep channels (cf. Reesink & Bridge, 2009; Ashworth *et al.*, 2011; Reesink *et al.*, 2014) related to a fluvial system possessing an overall high width to depth ratio (cf. McCabe, 1977; Bristow, 1993), which would accommodate the geometry of this element. The second-order bounding surface overlying the alternate-bar deposits and the associated change in lithofacies denote a change in flow conditions (Miall, 2010b). The uppermost deposits in these elements probably record the passage and accumulation of medium-scale sinuous-crested dunes possibly associated with an overall channel-fill succession (cf. McCabe, 1977). Such accumulations probably record a change in flow regime to turbulent flow conditions associated with reduced channel depth, indicative of channel-fill successions consisting of an evolution from sandy bedform, to alternate bar and back to sandy bedform (Fig. 10), which is comparable with the coarse-grained distributary model of McCabe (1977).

The characteristics of lithofacies *Spl/b,* which may underlie examples of this element, is indicative of upper-stage plane-bed accumulation, a common sedimentary structure in the upper parts of many channel deposits (Collinson, 1996). Upper-stage plane bed laminations are known to form in shallow flows on bar tops during falling-stage flow (Bristow, 1993; cf. Fidolini *et al.*, 2013). Such flows tend to subdue dune formation in favour of very low relief bedforms that give rise to planar laminations under conditions of laminar flow. Although falling-stage flow can be associated with subdued bedform migration and active vertical accretion (Ashworth *et al.*, 2011), it is also known to be associated with bar-top incision of up to 4 m (Bristow, 1993). As a result, minor chute channels develop on the upper surfaces of bars (cf. Ashworth *et al.*, 2011) in response to overflow from major channels undergoing drawdown and incision as the water level drops (Bristow, 1987). Such facies associations probably exhibit the stacking of relatively minor channels within major channels or the continuation of one channel succession and the instigation of a subsequent channel succession. Brierley (1991) and Ghinassi (2011) identify similar minor chute channels, which are suggested to form a diverse array of types including cut-offs and channels occupying swales, which may dissect the surface of a larger bar.

*Sandy bedform, mesoforms (SB)*

*Description:* Component lithofacies of this element are medium sandstone to granulestone with *ca* 2% small pebble content. Examples of this element are represented from bottom to top by a variable vertical succession of facies that record the accumulation of various mesoforms [Figs 5, 9 (log profiles E, F and J to Q) and 10; Table 1]. The lowermost facies in these elements is typically small-scale to medium-scale tabular cross-bedded sets (*Sl-hpx <2.0 m)* characterized by planar cross-bedded sets consisting of easterly dipping, medium-angle to high-angle-inclined (18˚ to 25˚) foresets forming >3.0 m wide and *ca* 0.4 m thick tabular cross-bedded sets. This facies is typically bounded at its top by a sub-horizontal, second-order, easterly dipping (*ca* 9˚) surface, and at its base by sub-horizontal, second-order, southerly dipping (*ca* 8˚) underlying surfaces. Overlying facies of small-scale trough cross-bedding (*Stsx <1.5 m)* are characterized by poorly defined <1.5 m wide and <0.3 m thick trough cross-bedded sets that are capped by an irregular, erosional scour surface and an associated lag of small to medium sized pebbles. Overlying facies are commonly characterized by <0.3 m thick, poorly defined planar cross-bedded sets, intermittent lags of small to medium sized pebbles (*Ss-lp-lag*) and a sharp and commonly erosional sub-horizontal and southerly dipping (≤8˚) overlying second-order surface. Overlying facies of large-scale trough cross-bedding (*Stlx >3.0 m)* are characterized by westerly dipping low-angle-inclined to medium-angle-inclined (10˚ to 18˚), *ca* 3 mm thick foresets arranged in shallow troughs that are >3.0 m wide and 0.5 m thick. Such facies may exhibit sub-horizontal westerly dipping (~*ca* 4˚) gradational second-order contacts with overlying sets. Uppermost in examples of this element are sets of medium-scale to large-scale tabular cross-bedding (*Sl-hpx <2.0 m)* characterized by packages consisting of poorly defined, westerly dipping, moderate-angle-inclined (10˚ to 20˚), graded (normal) foresets (fining-up from granulestone) arranged into >3.0 m wide and 0.5 m thick tabular cross-bedded sets. Within this facies, first-order reactivation surfaces are common. This facies exhibits a sharp, sub-horizontal, southerly dipping (*ca* 4˚) erosional overlying second-order surface, which defines the upper surface of the element. Trends from palaeocurrent data indicate that foresets and bounding surfaces associated with the lower facies present in examples of this element are mainly easterly trending, whereas uppermost facies

possess mainly westerly trending azimuths. Collectively the component lithofacies form elements that are up to 2.0 m thick, >10.0 m wide and >10.0 m long.

*Interpretation:* The various lithofacies that comprise this element are indicative of the migration and accumulation of dune-scale mesoforms that record the initial easterly migration of large, straight-crested dunes, and the later westerly migration of similar-sized sinuous and straight-crested dunes. The average preserved set thickness of *ca* 0.45 m, for facies *St*l*x >3.0 m* and *Sl-hpx <2.0 m,* suggests original mean dune heights of 1.0 to 1.6 m (Leclair, 2011), comparable to the Coleman (1969) description of megaripple bedforms in the Brahmaputra River, Bangladesh. Although Coleman (1969) noted that there was no relation between channel depth and the height of megaripples, a water depth of ≤3.0 to 4.8 m is envisaged for dune migration and aggradation (see Reesink & Bridge, 2009). In a study of the South Saskatchewan River, Cant & Walker (1978) demonstrated that dunes with a maximum height of 1.5 m developed during flood events within channels possessing a mean flow depth of 3.0 m, whereas deeper channels possessed larger dunes (cf. Reesink & Bridge, 2009; Ashworth *et al.*, 2011; Reesink *et al.*, 2014). Although flume observations by Coleman (1969) suggest that dune height may be less than or equal to the depth of water flowing over the dune, flume experiments by Reesink & Bridge (2009) demonstrate that the height and length of sand dunes increase with water depth and discharge rate. The highest and average dune heights are recorded at two-thirds and one-third of the water depth, respectively. Further, dune heights may be a function of water depth, rather than sediment supply (cf. Carling *et al.*, 2000). Studies of the Brahmaputra River by Coleman (1969) and Bristow (1987, 1993) and of the South Saskatchewan River by Ashworth *et al.* (2011) show that the majority of net bedform migration occurs during flood events, whereas the ensuing falling-flow stage results in net sediment deposition. This net deposition during falling-flow stage is responsible for altering channel flow in the immediate area of deposition, thereby resulting in localized thalweg migration and alterations in flow direction (cf. Coleman, 1969; Bristow 1987; Ashworth *et al.*, 2011). Such behaviour may account for the east to west alternation in palaeocurrent trends associated with examples of this element in the Lower Brimham Grit (Fig. 10). Furthermore, the lag deposit (*Ss-lp-lag*) and associated scour surface, and relative increase in bedform size related to lithofacies *St*l*x >3.0 m* and *Sl-hpx <2.0 m*, imply a temporal increase in palaeo-discharge and possibly an increased rate of dune migration and accumulation, probably facilitated by flood events (cf. Coleman, 1969; Bristow, 1987, 1993; Ashworth *et al.*, 2011). Such events probably facilitated the processes that gave rise to the distinct normal grading in the foresets associated with facies *Sl-hpx <2.0 m* in these elements, which are comparable to the graded foresets of facies *Sl-hpx >2.0 m* (see architectural element DA2 above). Lag deposits (*Ss-lp-lag*) may also denote the location of channel thalweg regions (Fidolini *et al.*, 2013; cf. Ghinassi *et al.*, 2014), thereby providing a useful indicator of the deepest, axial region of the channel (Ghinassi *et al.*, 2014). Such lag deposits may also be associated with relatively large bedforms (Reesink & Bridge, 2009; Ashworth *et al.*, 2011; Reesink *et al.*, 2014). First-order reactivation surfaces within facies *Sl-hpx <2.0 m* probably record: (i) relatively minor localized erosion or fluctuations in palaeocurrent direction (Miall, 2010b), possibly attributed to flow-stage oscillations (Collinson, 1970) due to flood events (Ashworth *et al.*, 2011); (ii) variations in bedform alignment (Haszeldine, 1983); or (iii) slip-face reworking (Collinson, 1996) by superimposed bedforms (Reesink & Bridge, 2007, 2009; Ashworth *et al.*, 2011). Smith (1972) observed graded planar cross-bedded foresets in transverse bars of the Platte River, Nebraska, which appear to be comparable to the normal grading in foresets

related to facies *Sl-hpx <2.0 m*. Smith (1972) noted that unstable lobes along the depositional margins of 3D transverse bars produced variable current directions and laterally variable foreset azimuth-dips. By contrast, the graded (normal) foresets associated with *Sl-hpx <2.0 m* do not exhibit significant along-strike variability in dip azimuth, which implies that they probably represent straight-crested (i.e. 2D) bedforms rather than 3D transverse bars. This element is best interpreted to represent the deposits of multiple sandy bedforms because it lacks characteristics associated with larger compound bars such as plane beds, ripples, down-current dipping cross-bedding, surfaces indicative of lateral accretion (cf. Bristow, 1993) and evidence for bedform superimpositioning (cf. Rubin & Carter, 2006); thus, there are no apparent structures to relate the preserved bedsets to the development of a larger bar complex. Comparisons with similar outcrop studies (e.g. Cant & Walker, 1976; Ashworth *et al.*, 2011; Reesink *et al.*, 2014) imply that the predominantly medium-scale to large-scale dunes related to this element were deposited within channel bases and not upon parent barforms.

*Lateral-accretion, macroform (LA)*

*Description:* Component lithofacies of this element are medium-grained sandstone to granulestone that are represented from bottom to top by a variable vertical succession of facies [Figs 5, 9 (log profiles J, L and O) and 10; Table 1]. In the lower part of these elements, small-scale horizontal sets (*Sl-hhs <1.0 m)* are characterized by southerly dipping, low-angle-inclined to high-angle-inclined (≤24˚) foresets and small-scale, *ca* 0.1 m thick, horizontal planar cross-bedded sets bounded by first-order surfaces. Packages of several sets are bounded by second-order surfaces that exhibit sharp, southerly dipping (*ca* 16˚), sub-horizontal and commonly erosional overlying contacts. Overlying facies of low-angle-sub-horizontal sets with oblique foresets *(Sl-hss-of <0.2 m)* are characterized by low-angle to medium-angle inclined (≤22˚) foresets and small-scale, <1.5 m wide and *ca* 0.1 m thick trough cross-bedded, sub-horizontal graded (normal) sets bounded by first-order surfaces defined by a basal coarse-grained component. Such facies exhibit foresets that are aligned obliquely with respect to their set bounding surfaces; for example, foreset and set azimuths trend at 144˚ and 181˚, respectively [Figs 9 (log profile J) and 10V]. Packages of several sets are bounded by third-order surfaces that exhibit sharp and commonly erosional, southerly dipping overlying contacts. Uppermost facies in examples of these elements are small-scale sub-horizontal sets (*Sl-hss <1.0 m)* characterized by medium-angle inclined (≤20˚) foresets and *ca* 0.1 m thick planar cross-bedded sub-horizontal sets bounded by first-order surfaces. Packages of several sets are bounded by second-order surfaces that exhibit sharp and southerly dipping overlying contacts. The lithofacies associated with this element may exhibit both southerly and westerly palaeocurrents and individual examples of these elements are up to 2.0 m thick, >10.0 m wide and >10.0 m long.

*Interpretation:* Examples of this element exhibit preserved features which possess palaeocurrent azimuth-dip relationships that indicate a combination of both downstream-accretion and lateral-accretion. Lateral-accretion elements are distinguished by facies that possess foreset azimuth data which dip obliquely to their respective first-order set bounding surfaces. Such combinations of downstream-accretion and lateral-accretion are likely to represent periods of falling-stage flow, whereby growth along bar margins is governed by lateral-accretion. The internal arrangements of

lithofacies within such examples record an initial south/south-westerly downstream migration and accumulation of straight-crested and sinuous-crested dunes. The average preserved set thickness of *ca* 0.1 m for sets suggests that the original mean dune heights were in the region of 0.2 to 0.35 m (Leclair, 2011). Hence, a water depth of ≤0.6 to 1.05 m is envisaged to accommodate dune migration and aggradation (see Reesink & Bridge, 2009). The coarser-grained component defining the first-order set bounding surface relating to *Sl-hss-of <0.2 m*, is probably due to a process of winnowing (cf. Collinson *et al.,* 2006), rather than to episodic deposition from suspension, or intermittent avalanching of fine-grained to coarse-grained sediments. Cant & Walker (1976) describe a facies similar to *Sl-hhs <1.0 m* and attribute it to migratory bedforms developed on the surface of larger sand flats, or towards the upper sections of a channel fill succession (cf. Reesink *et al.*, 2014); both scenarios are consistent with deposition in relatively shallow water (cf. Ashworth *et al.*, 2011). Similarly, Ghinassi *et al.* (2009) attribute horizontal bedding from fluvial sediments of the Alat Formation (Pleistocene Dandiero Basin, Eritrea) to downstream migration of longitudinal bars. Such bedforms are also associated with a series of distinct depositional episodes (Collinson *et al.,* 2006). During falling-flow stage conditions, large channel bedforms (for example, bars) may control the flow pattern of a channel at times when bars become increasingly exposed such that they gradually divide and divert the main channel flow around bar margins, rather than over bar surfaces (Collinson, 1970, 1996; cf. Reesink *et al.*, 2014). Areas adjacent to bar margins form topographic lows that may limit the falling-stage current flowing between bars (Collinson 1970; cf. Reesink *et al.*, 2014). Such arrangements may facilitate lateral accretion by promoting deposition along bar margins (Collinson, 1970, 1996). Therefore, an interpretation of facies *Sl-hhs <1.0 m* as a channel bar would support the interpretation of the deposition of facies *Sl-hss-of <0.2 m* as a component of lateral accretion; falling-flow stage would have facilitated the oblique migration of foresets down the margins of the bar towards an azimuth of 231˚, in contrast to the 181˚ azimuth associated with the migration of the set bounding surface (Fig. 10). The second-order bounding surface between *Sl-hhs <1.0 m* and *Sl-hss-of <0.2 m* and associated change in lithofacies denote a change in flow conditions (Miall, 2010b). Lithofacies associated with this element may also exhibit southerly dipping sub-horizontal erosional third-order overlying contacts. The erosional surface is consistent with the Miall (2010b) classification of third-order surfaces which may denote erosional surfaces within macroforms (for example, coset boundaries; cf. Ielpi *et al.*, 2014) or along the surface of minor bars or bedforms. Such erosional contacts are consistent with being generated during falling-flow stage along a bar margin, or front, as noted by (Collinson, 1970, 1996). During ensuing episodes of rising-flow stage, downstream currents apparently became increasingly influential and this favoured deposition and accretion along the downstream leading edge of the barform (cf. Collinson *et al.,* 2006). This interpretation is consistent with the deposition of the uppermost facies *Sl-hss <1.0 m*, which possesses downstream, southerly dipping foreset azimuths similar to lowermost facies *Sl-hhs <1.0 m* (Fig. 10), thereby indicating the restoration of downstream-accretion.

*Interdune (ID)*

*Description:* Component lithofacies of this element are coarse-grained sandstone to granulestone with 2 to 5% small pebble content that are represented from bottom to top by a distinctive vertical succession of facies [Figs 5, 9 (log profile L) and 10; Table 1]. Medium-scale to large-scale tabular cross-bedded facies (*Sl-hpx <2.0 m)* underlie interdune elements and are characterized by north-

westerly dipping, medium-angle-inclined (18˚ to 20˚), graded (normal) foresets forming >3.0 m wide and 0.9 m thick planar cross-bedded tabular sets. These facies are commonly bounded at their top by sharp horizontal second-order surface contacts. Overlying planar and horizontally laminated facies (*Spl/b)*, which represent the interdune itself, are characterized by <5 mm thick horizontal laminations arranged into a single *ca* 0.15 m thick horizontal set. Examples of such sets are bounded by second-order surfaces that exhibit sharp horizontal overlying contacts. Interdune elements are directly overlain by medium-scale to large-scale tabular cross-bedded facies (*Sl-hpx <2.0 m)* characterized by north-westerly dipping, medium-angle-inclined (18˚ to 22˚), graded (normal) foresets forming >3.0 m wide and 0.6 m thick planar cross-bedded tabular sets with a 10 to 15 mm thick layer of small pebbles forming a minor lag along the base of the set. The cross-bedded units that lie below and above the horizontally laminated interdune units of this element record predominately north-westerly palaeocurrents. Typical interdune elements are up to 1.0 m thick, >3.0 m wide and >3.0 m long.

*Interpretation:* The internal arrangement of lithofacies within examples of this element records small-scale (<0.2 m thick) horizontally laminated sets representing interdunes developed between relatively large medium-scale to large-scale tabular bedforms. Such planar and horizontally laminated sets probably represent interdune deposits generated during episodes of waning flow (low-flow stage). During the onset of low-flow stage it is likely that the relatively finer-grained interdune deposits continued to be transported whilst the migration of coarser-grained dunes ceased. As the channel flow continued to wane, so the interdune sediments gradually accumulated (cf. Collinson, 1996). Alternatively, the interdune deposit may denote upper-stage plane-bed accumulation, a common sedimentary structure in the upper parts of many channel deposits (Collinson, 1996). Because the migration of larger dunes was hindered during waning flow they may have contributed sediments which migrated over and accumulated in the interdune regions as relatively small-scale bedforms with higher celerities (cf. Carling *et al.*, 2000). Development of upper-stage plane-bed flow within interdune regions arose in response to falling water level that locally increased the palaeocurrent velocity within interdune regions. This development would have suppressed dune formation in favour of very low relief bedforms that give rise to planar laminations under conditions of laminar flow. The development of such planar laminations in interdune settings contrasts with the findings of studies that advocate the formation of backflow-ripples within the trough region ahead of an advancing dune, which are generated by a lee-side vortex (see Boersma *et al.*, 1968). The lithofacies that occur above and below interdune deposits (*Sl-hpx <2.0 m*) represent accumulations of medium-scale to large-scale, north-westerly migrating straight crested dunes which form second-order bounding surfaces with the interdune deposits. Although no palaeocurrent data were obtainable from the interdune deposits themselves, average palaeocurrent foreset azimuth data from the overlying (321˚) and underlying (340˚) planar cross-bedded sets imply that interdune deposition occurred under the influence of north-westerly directed palaeocurrents (Fig. 10). The average preserved set thickness of *ca* 0.6 m for the overlying facies suggests that the original mean dune height was in the region of 1.3 to 2.2 m (Leclair, 2011). Hence, a water depth of ≤3.9 to 6.6 m is envisaged to accommodate dune migration and aggradation (see Reesink & Bridge, 2009). As noted previously, Cant & Walker (1978) show that dunes with a maximum height of 1.5 m were detected during flood events within channels possessing a mean flow depth of 3.0 m. Such dunes probably formed in channel thalweg regions (cf. Ashworth *et al.*, 2011), where deeper

channels possessed larger dunes, which themselves were separated by flat-bedded interdune areas (cf. Reesink & Bridge, 2009; Ashworth *et al.*, 2011; Reesink *et al.*, 2014). Therefore, given the grain size and lag deposit associated with the overlying facies, it is likely that the interdune accumulated during low-stage flow, which preceded a flood event where the original mean channel flow depth may have been over 3.0 m.

## DEPOSITIONAL MODEL

It has long been recognized that the deposits of many braided fluvial systems comprise the following sedimentary characteristics: (i) a generally coarse-grained sediment composition (Coleman, 1969; Bristow, 1988); (ii) a predominance of down-current dipping cross-bedding (Bristow, 1988); (iii) an abundance of planar cross-bedding (Smith, 1972); (iv) evidence for lateral migration of in-channel bars and substantial proportions of an in-channel fill composed of sandy facies, rather than fine-grained facies indicative of vertical accretion (Cant & Walker, 1976); and (v) in sandy braided rivers, a predominance of in-channel barforms (both singular and compound bars) and in-channel fill deposits (Ashworth *et al.*, 2011). Similarities, however, between in-channel bar and fill successions may render such deposits indistinguishable from one another (see Ashworth *et al.*, 2011).

Such components are exhibited by the facies assemblages present in this study succession (Figs 6 to 13). Furthermore, meandering fluvial systems may evolve into braided systems through an increase in fluvial discharge which leads to the generation of multiple chute channels on point-bar top surfaces (Ghinassi, 2011). Examples of several well-known modern and ancient braided fluvial systems demonstrate that such systems are dominated by coarse sediments – I.e. sandy to gravel grade facies (Fig. 11A to E). However, the proportion of fine-grained deposits in such systems is variable. The modern Ganges and ancient Rio Vero Formation possess *ca* 20% fine-grained facies, whereas the Lower Brimham Grit, and modern Brahmaputra and Gash rivers possess 0 to 5% fine-grained facies (Fig. 11A to E). Although the fluvial systems show that transitions occur from both fine-grained facies to sandy facies, and vice versa, the examples illustrated imply that such systems are dominated by transitions towards sandy facies (Fig. 11A to E). Significantly, although highly cohesive channel banks promote channel stability (cf. Ghinassi, 2011), the absence of cohesive, fine-grained floodplain deposits in this study succession implies that the fluvial system was probably related to a fluvial setting where a high rate of delivery of sandy sediments facilitated channel bank and bar instability (cf. Collinson, 1996). Associations of facies and their occurrence as a distinctive suite of architectural elements record accumulation within a braided fluvial system. These associations are characterized by a broad channel belt within which mobile sandy barforms developed and migrated, and probably divided flow into multiple coevally active channels (cf. Ielpi *et al.*, 2014).

Detailed lithofacies and palaeocurrent analysis undertaken during this study (Figs 7 and 8) demonstrate the heterogeneity of lithofacies types present and their arrangement into a series of architectural elements. This heterogeneity is characterized by a complex style of stacking of sets and

cosets is indicative of the growth and migration of a series of barforms that accumulated in response to varying palaeocurrents and associated changes in discharge and flow regime within the fluvial system. Similarly, Reesink *et al.* (2014) attribute heterogeneity observed between bars within the Río Paraná (a large multi-channel river) to their respective age, size, form, developmental history, flow regime and sediment transport history. Within the Lower Brimham Grit, the lithofacies and architectural elements associated with such barforms are especially well-exposed at Locations 1 and 2 (Figs 2C and 8) and these representative sections are useful examples for the development of a detailed depositional model.

A predominantly south/south-easterly palaeocurrent is recorded early in the development of the sedimentary succession associated with Location 1 (Figs 7 and 9, log profiles F to L). At this locality, combined downstream-accretion and lateral-accretion associated with bar development is recorded. Migration of macroforms in the lower part of the successions arose in response to the net migration of channel barforms associated with south/south-easterly palaeocurrents, probably under conditions of relatively low to moderate amounts of sediment input. Such amounts of sedimentation are indicated by the following sedimentary characteristics: preservation of sets that are predominantly <0.2 m thick; erosion between sets implying subcritical climb whereby the rate of bedform migration greatly exceeded the component rate of vertical bedform accumulation (cf. Collinson *et al.*, 2006); an absence of bed sets that preserve topset deposits (cf. Bristow, 1993).

Architectural elements that characterise the lower 2 m of the succession consist of predominantly downstream-accretion macroforms (DA1) which underlie lateral-accretion macroforms (LA); both macroform types are characterized predominantly by southerly migrating, sinuous-crested dunes. Subsequent overlying facies consist of planar cross-bedded sandy bedforms which denote a change in the palaeocurrent from a southerly to south-easterly direction.

By contrast, the upper 10 m of the succession records a westerly palaeocurrent regime associated with multiple channel incisions and the accumulation of more substantial sandy bedforms associated with a combination of both downstream-accretion and lateral-accretion of in-channel barforms [Figs 8 (panel D) and 9 (log profile H)]. At Locality 1, architectural elements that characterise the upper part of the succession are represented by a series of three stacked channel (CH) elements (up to 4 m thick) that can be traced laterally for 70 m (Fig. 12). These channel elements vary both laterally and vertically with regard to the content of their respective component facies [Figs 8 (panels A to D), 9 (log profiles G to I) and 12]. The base of each channel element is denoted by variations in palaeocurrent direction and a change in lithofacies, in some instances signified solely by a variation in grain composition or size. Such observations are similar to features described by Ghinassi (2011) which demonstrates that distinct changes in grain-size denote unit boundaries within a sedimentary succession. The abrupt adjustment in the style from downstream-accretion or lateral-accretion lithofacies, with set thicknesses <0.2 m, to more substantial sandy bedforms that are each 0.5 to 0.9 m thick and characterized by coarser grain components probably record flood events that induced bedform migration along the channel system, whereby subsequent falling-stage flow resulted in net

sediment accumulation (Coleman, 1969; Bristow 1987; 1993; cf. Ashworth *et al.*, 2011). The observed variation in overall palaeocurrent, from south/south-easterly in the lower part of the succession to westerly in the upper part, is attributed to sediment deposition during falling-stage flow that induced a localized shift in channel configuration and associated flow pattern in the immediate area of deposition in response to thalweg migration (cf. Coleman, 1969; Bristow 1987; cf. Ashworth *et al.*, 2011). Thus, a distinct change in the overall orientation of the architectural elements that give rise to the preserved succession is recognized.

Palaeocurrent readings [Figs 7 and 9 (log profiles M to Q); Location 2] collectively reveal a range of bedform migration directions probably related to flood events or migrating channel bars. Flood events are probably recorded by the presence of relatively large sandy bedform components (cf. Cant & Walker, 1978; Ashworth *et al.*, 2011; Reesink *et al.*, 2014) and a variation in palaeocurrent direction (cf. Coleman, 1969; Bristow, 1987). By contrast, a succession of smaller (<0.2 m thick) sets probably represent channel bar migration under non-flood conditions (cf. Cant & Walker, 1976; Miall, 2010b; Ashworth *et al.*, 2011). The palaeocurrent data range in a distinctive way as a result of an increase in palaeocurrent velocity, as implied by the presence of relatively large sandy bedforms, pebble lag and coarser-grained components (see Fig. 9, log profile P). Relatively large and small pebble lags are probably representative of scouring (cf. Miall, 2010b) and winnowing processes (cf. Collinson *et al.*, 2006), respectively, or a combination of both (cf. Collinson, 1996), which may also denote thalweg regions (Fidolini *et al.*, 2013; cf. Ghinassi *et al.*, 2014) within deposits. Alternatively, lag deposits may also be associated with barhead deposition and the basal fractions of successive bars (Ashworth *et al.*, 2011).

Three-hundred metres to the north of Location 2, the base of the section at Location 1 corresponds to the top of the section at Location 2 based on lateral tracing of key stratal surfaces. The base of Location 1 and the top of Location 2, both occur at an elevation of *ca* 280 m (Fig. 13) and both possess foreset and set palaeocurrent azimuths that dip in a south/south-easterly direction (Fig. 9; for example, log profiles I and P, respectively). Thus, in contrast to Locality 1, a south/south-easterly palaeocurrent is exhibited late in the development of the sedimentary succession associated with Locality 2, and a westerly palaeocurrent is exhibited early in the development of the succession. These palaeocurrents demonstrate that the sedimentary succession related to the study area was influenced by a complex flow regime, whereby flow direction varied markedly over distances of just a few hundred metres, probably as a consequence of flood events and associated rising-stage and falling-stage flows acting on transient bars. Observed relationships also demonstrate that the deposits at both Locations 1 and 2 form part of a genetically related stratigraphic sedimentary succession: the channel-bar feature at the bottom of Location 1 is comparable to a similar feature at the top of Location 2, *ca* 300 m to the south. Two possible interpretations for these observations are: (i) both features formed part of an extensive downstream-accretion macroform; and (ii) two separate and somewhat smaller but morphologically similar macroforms were present within a comparatively broad channel in a manner similar to that documented from the Brahmaputra River, Bangladesh (Bristow, 1987, 1993) and the South Saskatchewan River, Canada (Ashworth *et al.*, 2011).

Pseudo-3D box panels (Fig. 13, Locations 1 and 2) have been developed to portray the relative position and relationship of the sedimentary graphic log profiles (Fig. 9) so as to infer the position and orientation of the primary fluvial channels present in the succession (blue shaded areas). The log profiles associated with Locations 1 and 2 reveal a pattern of juxtaposition of architectural elements that is consistent with a repeatedly variable braided fluvial system, facilitated by flood events. Figure 11 exhibits three bar charts (F to H) which indicate that channel elements (CH) dominate the succession and form *ca* 50% of the total recorded thickness from log profiles E to Q; sandy bedforms and downstream-accretion elements (DA1) each comprise *ca* 23% of the succession; downstream-accretion and oblique-accretion (DA2), lateral-accretion (LA) and interdune (ID) elements comprise *ca* 3%, 2.5% and <0.5% of the remaining succession, respectively. An example of element distribution is shown in Fig. 11I, which is a composite of log profiles P, J and E (Locations 1 and 2, see Figs 7, 9 and 13). Figure 11I forms a near-continuous, 32 m thick section of the uppermost part of the *ca* 50 m Lower Brimham Grit succession present at the Brimham Rocks study area. Figure 11I also includes an indication of sub-facies associations that make up the architectural elements and depicts correlated mean palaeocurrent data, which provide an example of palaeocurrent variations between Locations 1 and 2 (see above).

The relationships described above are consistent with a fluvial system characterized by both stacked and laterally migrating channels that were broad and possessed variable channel depths [Figs 9 (log profiles E and G to Q) and 12]. Channel elements are identified primarily from distinct variations in palaeocurrents and facies associations in packages delineated by distinctive bounding surfaces. The fill of each channel element comprises mainly large-scale sandy bedforms (SB), small-scale migratory bedforms (DA1 and/or LA) or a combination thereof. Although sandbody preservation implies that the depositional environments for both the stacked and laterally migrating channels were influenced by low rates of aggradation, avulsion and incision, migration rates varied from low to moderate, respectively (cf. Bristow, 1996; Figs 12 and 13). Lateral tracing of fifth-order bounding surfaces demonstrates the juxtaposition of relatively low-angle channel base contacts on to underlying units. At the base of the succession (Location 2), successive channel elements are offset, whereas towards the top of the succession (Location 1) channel elements are vertically stacked (Figs 12 and 13). Such observations suggest that the depositional environment evolved from a laterally migrating to a stacked fluvial channel system.

Bounding surfaces contained within the channel elements reveal whether the fill of the channels was related to one or more of the following: (i) small-scale (<0.2 m thick) cross-bedded units that represent continuous migration of a series (train) of in-channel bedforms (first-order set bounding surfaces; Miall, 2010b); (ii) migration and aggradation of larger dunes that exhibit evidence for variation in lithofacies evolution related to changing flow conditions and direction (second-order coset bounding surfaces; Miall, 2010b); (iii) erosional cross-cutting surfaces within macroforms representative of growth increments (third-order bounding surfaces; Miall, 2010b; Ielpi *et al.*, 2014); and (iv) erosional cross-cutting surfaces along the surface of minor bars or bedforms indicative of falling-stage flow (also third-order bounding surfaces; Miall, 2010b).

Although the data highlight the complexity of the palaeocurrents associated with the succession, there appears to be a level of consistency with regard to the deposition of very coarse-grained to granular sandy bedforms. In the studied interval, such sandy bedform deposits tend to record migration in a predominantly westerly direction, whereas medium-grained to coarse-grained deposits of sandy bedforms and of downstream-accretion and lateral-accretion elements (DA1 and LA, respectively) tend to migrate towards a south-easterly or south-westerly direction. Figure 14 demonstrates the likely arrangement of in-channel barforms, the reconstructed arrangement of which account for the trends in the observed palaeocurrent data collated from two sedimentary graphic log profiles at Location 2. In the lower part of the succession (log profile O, Fig. 14), which accumulated prior to channel incision and thalweg migration, palaeocurrent data from foreset azimuths record dune migration toward the south/south-west. By contrast, following the episode of channel incision and thalweg migration, palaeocurrent data from foreset azimuths record dune migration mainly toward the north/north-west. In the upper part of the succession, accumulated sets and associated cosets are delineated by bounding surfaces that record growth and migration of barforms perpendicular to the axis of the main channel margin (i.e. laterally with respect to the inferred trend of the channel bank). By contrast, palaeocurrent data from foresets record superimposed dune migration in a direction close to parallel to the trend of the main channel axis but perpendicular to the above-mentioned direction of set and coset migration. Thus, the preserved deposits record progressive growth of lateral accretion macroforms as point bars.

Although downstream-accretion and lateral-accretion deposits are associated with both southerly and westerly palaeocurrents at Location 1, the majority of sandy bedform deposits are related to westerly palaeocurrents. Such sandy bedforms are probably related to flood events and their associated rising and falling-flow stage palaeocurrents. Hence, although the deposition of the sedimentary successions associated with Locations 1 and 2 appears to be related to variable palaeocurrents, the deposition of large sandy bedforms is predominantly associated with westerly palaeocurrents.

Figure 15 proposes a broader depositional model for the succession, within which the detailed sedimentary observations related to Locations 1 and 2 are shown. The model consists of two main interpretations (pre-flood and post-flood events) and demonstrates how the depositional environment was probably influenced by two distinct flow regimes. The model depicts how the channelized fluvial system of the upper-delta plain developed a varied and complex flow direction, and volume and rate of sediment input as a function of the autogenic behaviour of bars and channels in an active braided fluvial system susceptible to repeated channel incision and thalweg migration. The general lack of cohesive sediment within the fluvial system resulted in the development of unstable banks that were vulnerable to reworking during and in the immediate aftermath of flood events. Major channel incision events may have potentially arisen in response to allogenic factors, including tectonic tilting of the land surface associated with movement on the nearby North Craven Fault.

## DISCUSSION

The depositional environment associated with emplacement of the Brimham Grit is related to development of an upper-delta plain braided fluvial system in which barform elements underwent both lateral-accretion and downstream-accretion associated with migration of sandy bedforms and channels. Within the study area, this interpretation is consistent with the predominantly coarse grain size associated with the Lower Brimham Grit and relative absence of ripple sets that are typically associated with finer-grained fluvial successions. This implies a relatively proximal, rather than distal, depositional setting on the delta plain.

The braided fluvial system probably flowed in a relatively open incised palaeovalley that formed within a fault relay zone associated with the North Craven Fault (Fig. 4B and C; cf. Larsen, 1988; Reid, 1996; Gobo *et al.*, 2014). This fault relay zone formed a ramp that acted as a transfer zone which transmitted displacement between overstepping normal fault segments with similar dip directions (Peacock & Sanderson, 1994). Fault relays are known to be associated with fluvial valley incision, generation of accommodation space and local diversion of rift-margin drainage systems in several rift-basin settings (e.g. Gobo *et al.*, 2014). Might the incised valley and other erosional surfaces recognized internally within the Lower Brimham Grit studied here have arisen as a consequence of tectonic activity at the basin margin?

The *ca* 4 m deep channel incision observed at Location 1 (Fig. 12, 2$^{nd}$ channel element) may have been generated as a result of allogenic tectonic activity. Such activity is likely because the North Craven Fault system (Fig. 4B) is located only *ca* 1 km to the north/north-west of Brimham Rocks (O. Wakefield, personal communication) and is known to have been active at the time of accumulation (Thompson, 1957). Indeed, Thompson (1957) demonstrated that, following a period of tectonic activity and uplift of the region south of the North Craven Fault, tectonic activity along the North Craven Fault led to the gradual and progressive downward displacement of the region south of the fault by around 122 m, during the episode of deposition of the Lower Brimham Grit. Such tectonic activity would probably have governed the amount of local subsidence and therefore available accommodation (cf. Gawthorpe *et al.*, 1994; Fidolini *et al.*, 2013). Waters & Condon (2012) imply that during this period the region was not influenced by major marine transgression or region-wide incision. The authors argue for relatively stable eustatic sea-level conditions associated with a protracted interglacial period (*ca* 321.5 to 319.5 Ma). Although speculative, given deposition of the Lower Brimham Grit was completed within *ca* 250 kyr, displacement of the region south of the North Craven Fault by around 122 m, during this period, would have generated accommodation at a time-average rate of *ca* 0.5 m per 1000 years. Downward displacement of the hangingwall along the southern margin of the North Craven Fault may have generated lateral tilting along the fault relay ramp system around Pateley Bridge leading to development of a topographic low towards the fault (Fig. 4B and C; cf. Peacock & Sanderson, 1994; Kane *et al.*, 2010; Fidolini *et al.*, 2013). Such lateral tilting may account for the switching from predominantly southerly to westerly palaeocurrents demonstrated in this study (cf. Reid, 1996; Gobo *et al.*, 2014). Alternatively, other minor and localized variations in palaeocurrent may be attributed to autogenic processes such as seasonal

flood events and locally complex patterns of barform arrangement. Hence, it is likely that southerly migrating channel elements correspond with the axial course of the braided fluvial system associated with the deposition of the Lower Brimham Grit; whereas westerly migrating channel elements may be related more to lateral tilting (cf. Kane *et al.*, 2010; Fidolini *et al.*, 2013) and seasonal flood events.

The driver for the generation of the preserved (*ca* 4.0 m deep) remnant of the channel incision observed at Location 1 (Fig. 12, 2$^{nd}$ channel element) could be related to either anallogenic mechanism (for example, eustasy, tectonic activity or differential rates of basin subsidence all of which might lead to local changes in the gradient of the delta plain) or an autogenic mechanism (for example, major channel avulsion, major flood event) or a combination of factors. Eustatic fall in sea-level could have potentially generated the incised channel, although such an event is unlikely given the relatively stable sea-level episode implied by Waters & Condon (2012). Channel incision may be attributed to activity on the North Craven Fault system (see Thompson, 1957; Reid, 1996). Such activity could also facilitate major channel avulsion (cf. Kane *et al.*, 2010; Fidolini *et al.*, 2013), which could generate a 4 m deep channel incision. Unless linked to tectonic activity, gradual subsidence is unlikely to have generated a deep incision; the underlying deposits possess generally horizontal contacts and do not appear to exhibit any signs of differential tilting and the generation of an angular discordance. Palaeocurrent data acquired from both above and below the channel base imply a generally westerly palaeocurrent, which would not be expected had the system undertaken a major avulsion. Although flood events may also generate incised channels, the deposits associated with the incised channel are similar to other deposits that are not related to deep channel incisions, which suggests that a rapid increase in discharge associated with a flood was not, on its own, likely to have facilitated channel incision. Of the factors listed here, incision associated with tectonic activity, possibly in conjunction with other events such as flooding, is considered most likely to have been responsible for the generation of the incision surface.

Palaeocurrent data collated from the Lower Brimham Grit at Brimham Rocks are consistent with sediment delivery via fluvial systems that passed from the Cleveland Basin towards the Harrogate and Craven Basins (cf. Martinsen, 1990), which are situated to the east/north-east, south-east and south-west of Brimham Rocks, respectively (Fig. 4B). The tectonically active North Craven Fault system (cf. Thompson, 1957) and its associated fault relay zone (cf. Reid, 1996; Gobo *et al.*, 2014) probably directed the fluvial system towards the Harrogate and Craven Basins. Also, fault activity could conceivably account for gradual but progressive channel-bar and sandy bedform migration towards the north-west, as indicated by palaeocurrent data.

## CONCLUSIONS

Data and results from this work form a valuable tool for comparative study of analogous fluvial systems and preserved successions, in both modern and ancient settings, which do not possess the unique three-dimensional characteristics of the outcrops of the Lower Brimham Grit at Brimham

Rocks. Such characteristics yield exceptional detail with regard to internal lithofacies associations and facilitate interpretations of how the juxtaposition of facies and architectural elements, within a depositional model, act to form the fundamental components of an ancient upper-delta plain braided fluvial succession, thereby improving current understanding and knowledge of such systems. The succession studied is dominated by both vertically and laterally arranged channel elements that are themselves filled primarily by large-scale sandy bedforms (bars) or small-scale migratory bedforms, or a combination thereof. Although the distribution of palaeocurrent data, facies associations and the arrangement of architectural elements are consistent with trends typical of sandy braided fluvial systems, the three-dimensional nature of the outcrops has enabled the complex history of evolution of the sedimentary system to be discerned, including documentation of the style of growth of bar elements via lateral accretion. Furthermore, this study also demonstrates how accumulation of the Lower Brimham Grit was probably influenced by externally forced tectonic activity related to movement on basin-bounding faults, and flood events driven by climatic control in a distant hinterland.

## ACKNOWLEDGEMENTS

Adrian and Joseph Soltan are thanked for their assistance with field data collection and Luca Colombera is thanked for his assistance with provision of supporting data from the Fluvial Architecture Knowledge Transfer System (FAKTS). This manuscript has benefitted from the constructive review comments made by Gary Hampson, Arjan Reesink, Oliver Wakefield and Charlie Bristow. This research was supported by funding from Areva, BHPBilliton, ConocoPhillips, Murphy Oil, Nexen, Saudi Aramco, Shell, Tullow Oil, Woodside and YPF through their sponsorship of the Fluvial & Eolian Research Group at the University of Leeds.

## REFERENCES

**Abdullatif, O.M.** (1989) Channel-fill and sheet-flood facies sequences in the ephemeral terminal River Gash, Kassala, Sudan. *Sedimentary Geology*, **63**, 171-184.

**Allen, J.R.L.** (1982) *Developments in Sedimentology 30A. Sedimentary structures, their character and physical basis. Volume 1*. Elsevier, Amsterdam, 593 pp.

**Allen, J.R.L.** (1983) Studies in fluviatile sedimentation: Bars, Bar-complexes and sandstone sheets (low-sinuosity braided streams) in the Brownstones (L. Devonian), Welsh Borders. *Sedimentary Geology*, **33**, 237-293.

**Arthurton, R.S.** (1983) The Skipton Rock Fault – an Hercynian wrench fault associated with the Skipton Anticline, northwest England. *Geological Journal*, **18**, 105-114.

**Arthurton, R.S.** (1984) The Ribblesdale fold belt, NW England – a Dinantian-early Namurian dextral shear zone. *Geological Society, London, Spec. Publ.,* **14**, 131-138.

**Arthurton, R.S., Johnson, E.W.** and **Mundy, D.J.C.** (1988) *Geology of the country around Settle*.

Memoir of the British Geological Survey, sheet 60 (England and Wales), 147 pp.

**Ashworth, P.J., Sambrook Smith, G.H., Best, J.L., Bridge, J.S., Lane, S.N., Lunt, I.A., Reesink, A.J.H., Simpson, C.J.** and **Thomas, R.E.** (2011) Evolution and sedimentology of a channel fill in the sandy braided South Saskatchewan River and its comparison to the deposits of an adjacent compound bar. *Sedimentology*, **58**, 1860-1883.

**Best, J.L., Ashworth, P.J., Bristow, C.S.** and **Roden, J.** (2003) Three-dimensional sedimentary architecture of a large, mid-channel sand braid bar, Jamuna River, Bangladesh. *Journal of Sedimentary Research*, **73**, No. 4, 516-530.

**Bhattacharya, J.P.** (2006) Deltas. In: *Facies Models Revisited* (Eds H.W. Posamentier and R.G. Walker), *SEPM Spec. Publ.*, **84**, 237-292.

**Bhattacharya, J.P.** (2010) Deltas. In: *Facies Models 4* (Eds N.P. James and R.W. Dalrymple), *Geological Association of Canada*, 233-264.

**Boersma, J.R., Van De Meene, E.A.** and **Tjalsma, R.C.** (1968) Intricated cross-stratification due to interaction of a mega ripple with its lee-side system of backflow ripples (upper-pointbar deposits, Lower Rhine). *Sedimentology*, **11**, 147-162.

**Bridge, J.S.** (1985) Palaeochannel patterns inferred from alluvial deposits: a critical evaluation. *Journal of Sedimentary Petrology*, **55**, 579-589.

**Bridge, J.S.** (2003) *Rivers and Floodplains: Forms, Processes, and Sedimentary Record*. Blackwell Science, Oxford, 491 pp.

**Brierley, G.J.** (1991) Floodplain sedimentology of the Squamish River, British Columbia: relevance of element analysis. *Sedimentology*, **38**, 735-750.

**Bristow, C.S.** (1987) Brahmaputra River: Channel Migration and Deposition. In: *Recent Developments in Fluvial Sedimentology* (Eds F.G. Ethridge, R.M. Flores and M.D. Harvey), *SEPM Spec. Publ.,* **39**, 63-74.

**Bristow, C.S.** (1988) Controls on the sedimentation of the Rough Rock Group (Namurian) from the Pennine Basin of northern England. In: *Sedimentation in a synorogenic basin complex; the Upper Carboniferous of Northwest Europe* (Eds B.M. Besly and G. Kelling), pp. 114-131. Blackie, Glasgow.

**Bristow, C.S.** (1993) Sedimentary structures exposed in bar tops in the Brahmaputra River, Bangladesh. In: *Braided Rivers* (Eds J.L. Best and C.S. Bristow), *Geological Society, London, Spec. Publ.*, **75**, 419 pp.

**Bristow, C.S.** (1996) Reconstructing fluvial channel morphology from sedimentary sequences. In: *Advances in fluvial dynamics and stratigraphy* (Eds P.A. Carling and M.R. Dawson), pp. 351-371. Wiley, Chichester, England.

**British Geological Survey** (2008) Modified British Geological Survey Timeline. Downloaded from: http://www.bgs.ac.uk/downloads/home.html - accessed 31/12/08.

**Cain, S.A.** (2009) *Sedimentology and stratigraphy of a terminal fluvial fan system: the Permian Organ Rock Formation, South East Utah*. Unpublished Doctoral thesis, Keele University.

**Cain, S.A.** and **Mountney, N.P.** (2009) Spatial and temporal evolution of a terminal fluvial fan system: the Permian Organ Rock Formation, South-east Utah, USA. *Sedimentology*, **56**, 1774-1800.

**Cant, D.J.** and **Walker, R.G.** (1976) Development of a braided-fluvial facies model for the Devonian Battery Point Sandstone, Québec. *Canadian Journal of Earth Sciences*, **13**, 102-119.

**Cant, D.J.** and **Walker, R.G.** (1978) Fluvial processes and facies sequences in the sandy braided South Saskatchewan River, Canada. *Sedimentology*, **25**, 625-648.

**Carling, P. A., Gölz, E., Orr, H. G. and Radecki-Pawlik, A.** (2000) The morphodynamics of fluvial sand dunes in the River Rhine, near Mainz, Germany. I. Sedimentology and morphology. *Sedimentology*, **47**, 227-252.

**Coleman, J.M.** (1969) Brahmaputra River channel processes and sedimentation. *Sedimentary Geology*, **3**, 129-239.

**Collinson, J.D.** (1970) Bedforms of the Tana River, Norway. *Geografiska Annaler*, **52**, No. 1, 31-56.

**Collinson, J.D.** (1988) Controls on Namurian sedimentation in the Central Province basins of northern England. In: *Sedimentation in a synorogenic basin complex; the Upper Carboniferous of Northwest Europe* (Eds B.M. Besly and G. Kelling), pp. 85-101. Blackie, Glasgow.

**Collinson, J.D., Holdsworth, B.K., Martinsen, O.J.** and **Bristow, C.S.** (1990) *Namurian Delta Systems of the Pennine area*. Compiled for the 13th International Sedimentological Congress, Nottingham U.K, Field Guide, **14**, 1-24.

**Collinson, J.D.** (1996) Alluvial Sediments. In: *Sedimentary Environments, Processes, Facies and Stratigraphy* (Ed. H.G. Reading), 3rd edn, pp.37-82. Blackwell Science, Oxford.

**Collinson, J.D., Mountney, N. P.** and **Thompson, D. B.** (2006) *Sedimentary Structures*. 3rd edn, Terra Publishing, Harpenden, 292 pp.

**Colombera, L., Mountney, N.P. and McCaffrey, W.D.** (2012a) A relational database for the digitization of fluvial architecture: concepts and example applications. *Petroleum Geoscience*, **18**, 129-140.

**Colombera, L., Felletti, F., Mountney, N.P. and McCaffrey, W.D.** (2012b) A database approach for constraining stochastic simulations of the sedimentary heterogeneity of fluvial reservoirs. *American Association of Petroleum Geologists Bulletin*, **96**, 2143-2166.

**Colombera, L., Mountney, N.P. and McCaffrey, W.D.** (2013) A quantitative approach to fluvial facies models: Methods and example results. *Sedimentology*, **60**, 1526-1558.

**Cooper, A.H.** and **Burgess, I.C.** (1993) *Geology of the country around Harrogate*. Memoir of the British Geological Survey, sheet 62 (England and Wales), 105 pp.

**Cope, J.C.W., Guion, P.D., Sevastopulo, G.D.** and **Swan, A.R.H.** (1992) Carboniferous. *Geological Society of London, Memoirs*, **13**, 67-86.

**Corfield, S.M., Gawthorpe, R.L., Gage, M., Fraser, A.J.** and **Besly, B.M.** (1996) Inversion tectonics of the Variscan foreland of the British Isles. *Journal of the Geological Society, London*, **153**, 17-32.

**Dale, R.E.** (2011) Global seal level control on sedimentation during the Carboniferous across the British Isles. Unpublished Doctoral thesis, University of Leeds.

**Davydov, V.I., Crowley, J.L., Schmitz, M.D.** and **Poletaev, V.I.** (2010) High-precision U–Pb zircon age calibration of the global Carboniferous time scale and Milankovitch band cyclicity in the Donets Basin, eastern Ukraine. *Geochemistry, Geophysics, Geosystems*, **11**, 1-22.

**Dunham, K.C.** and **Wilson, A.A.** (1985) *Geology of the Northern Pennine Orefield, Volume 2, Stainmore to Craven*. Economic Memoir of the British Geological Survey, sheets 40, 41, 50 and parts of 31, 32, 51, 60 and 61, New Series (England and Wales), British Geological Survey, Nottingham, 247 pp.

**Edina Digimap** (2013) © Crown Copyright/database right 2013. An Ordnance Survey/EDINA supplied service.

**Elliott, T.** (1989) Deltaic systems and their contribution to an understanding of basin-fill successions. *Geological Society, London, Spec. Publ.*, **41**, 3-10.

**Fidolini, F., Ghinassi, M., Aldinucci, M., Billi, P., Boaga, J., Deiana, R.** and **Brivio, L.** (2013) Fault-sourced alluvial fans and their interaction with axial fluvial drainage: An example from the Plio-Pleistocene Upper Valdarno Basin (Tuscany, Italy). *Sedimentary Geology*, **289**, 19-39.

**Fielding, C.R.** (1985) Coal depositional models and the distinction between alluvial and delta plain environments. *Sedimentary Geology*, **42**, 41-48.

**Fraser, A.J.** and **Gawthorpe, R.L.** (1990) Tectonic Events Responsible for Britain's Oil and Gas Reserves. *Geological Society, London, Spec. Publ*., **55**, 49-86.

**Fraser, A.J.** and **Gawthorpe, R.L.** (2003) Palaeogeography and Facies Evolution. In: *An Atlas of Carboniferous Basin Evolution in Northern England*. *Geological Society, London, Memoirs*, **28**, 27-49.

**Galloway, W.E.** (1975) Process framework for describing the morphologic and stratigraphic evolution of deltaic depositional systems. In: *Deltas, Models of Exploration* (Ed. M.L. Broussard), *Houston Geological Society, Houston*, 87-98.

**Gawthorpe, R.L.** (1987) Tectono-sedimentary evolution of the Bowland Basin, N England, during the Dinantian. *Journal of the Geological Society*, **144**, 59-71.

**Gawthorpe, R.L., Gutteridge, P.** and **Leeder, M.R.** (1989) Late Devonian and Dinantian basin evolution in northern England and North Wales. In: *The Role of Tectonics in Devonian and Carboniferous Sedimentation in the British Isles* (Eds R.S. Arthurton, P. Gutteridge and S.C. Nolan), *Yorkshire Geological Society Occasional Publications*, **6**, 1-23.

**Gawthorpe, R.L., Fraser, A.J.** and **Collier, R.E.LI.** (1994) Sequence stratigraphy in active extensional basins: implications for the interpretation of ancient basin-fills. *Marine and Petroleum Geology,* **11**, 642-658.

**Gawthorpe, R.L.** and **Leeder, M.R.** (2000) Tectono-sedimentary evolution of active extensional basins. *Basin Research*, **12**, 195–218.

**Geehan, G.** and **Underwood, J.** (1993) The use of length distributions in geological modelling. In: *The Geological Modelling of Hydrocarbon Reservoirs and Outcrop Analogues* (Eds S.S. Flint and I.D. Bryant), *Int. Assoc. Sedimentol. Spec. Publ.,* **15**, 205-212.

**Ghazi, S.** and **Mountney, N.P.** (2009) Facies and architectural element analysis of a meandering fluvial succession: The Permian Warchha Sandstone, Salt Range, Pakistan. *Sedimentary Geology*, **221**, 99-126.

**Ghinassi, M., Libsekal, Y., Papini, M.** and **Rook, L.** (2009) Palaeoenvironments of the Buia Homo site: High-resolution facies analysis and non-marine sequence stratigraphy in the Alat formation (Pleistocene Dandiero Basin, Danakil depression, Eritrea). *Palaeogeography, Palaeoclimatology, Palaeoecology*, **280**, 415–431.

**Ghinassi, M.** (2011) Chute channels in the Holocene high-sinuosity river deposits of the Firenze plain, Tuscany, Italy. *Sedimentology*, **58**, 618-642.

**Ghinassi, M., Nemec, W., Aldinucci, M., Nehyba, S., Özaksoy, V.** and **Fidolini, F.** (2014) Plan-form evolution of ancient meandering rivers reconstructed from longitudinal outcrop sections. *Sedimentology,* **61**, 952-977.

**Gilligan, A.** (1919) The petrography of the Millstone Grit of Yorkshire. *Quarterly Journal of the Geological Society, London*, **75**, 251-296.

**Gobo, K., Ghinassi, M., Nemec, W.** and **Sjursen, E.** (2014) Development of an incised valley-fill at an evolving rift margin: Pleistocene eustasy and tectonics on the southern side of the Gulf of Corinth, Greece. *Sedimentology,* **61**, 1086-1119.

**Google Earth** (2013) 2010 Google Earth image of Brimham Rocks; downloaded from Google Earth on 05th March 2013.

**Guion, P.D., Gutteridge, P.** and **Davies, S.J.** (2010) Carboniferous sedimentation and volcanism on the Laurussian margin. In: *Geological History of Britain and Ireland*. (Eds N.H. Woodcock and R.A. Strachan), pp. 227-270. Blackwell Science.

**Hallsworth, C.R., Morton, A.C., Claoué-Long, J.** and **Fanning, C.M.** (2000) Carboniferous sand provenance in the Pennine Basin, UK: constraints from heavy mineral and detrital zircon age data. *Sedimentary Geology*, **137**, 147-185.

**Hallsworth, C.R.** and **Chisholm, J.I.** (2008) Provenance of late Carboniferous sandstones in the Pennine Basin (UK) from combined heavy mineral, garnet geochemistry and palaeocurrent studies. *Sedimentary Geology*, **203**, 196-212.

**Haszeldine, R.S.** (1983) Descending Tabular Cross-Bed Sets and Bounding Surfaces from a Fluvial Channel in the Upper Carboniferous Coalfield of North-East England. In: *Modern and Ancient Fluvial Systems* (Eds J.D. Collinson and J. Lewin), *Int. Assoc. Sedimentol. Spec. Publ.,* **6**, 449-456.

**Hunter, A.** (2001) Palaeogeographic Map Booklet. In: SXR260, *Geological History of the British Isles*. The Open University, Milton Keynes, 16 pp.

**Ielpi, A., Gibling, M.R., Bashforth, A.R., Lally, C., Rygel, M.C.** and **Al-Silwadi, S.** (2014) Role of vegetation in shaping Early Pennsylvanian braided rivers: Architecture of the Boss Point Formation, Atlantic Canada. *Sedimentology,* **61**, 1659-1700.

**Jones, S.J., Frostick, L.E.** and **Astin, T.R.** (2001) Braided stream and flood plain architecture: The Rio Vero Formation, Spanish Pyrenees. *Sedimentary Geology*, **139**, 229-260.

**Jones, T.W.** (1943) The geology of the Beamsley Anticline. *Proceedings of the Leeds Philosophical Society*, **4**, Part 2, 146-166.

**Kane, I.A., Catterall, V., McCaffrey, W.D. and Martinsen, O.J.** (2010) Submarine channel response to intrabasinal tectonics: The influence of lateral tilt. *American Association of Petroleum Geologists Bulletin*, **94**, 189-219.

**Kirby, G.A., Baily, H.E., Chadwick, R.A., Evans, D.J., Holliday, D.W., Holloway, S., Hulbert, A.G., Pharaoh, T.C., Smith, N.J.P., Aitkenhead, N.** and **Birch, B.** (2000) *The structure and evolution of the Craven Basin and adjacent areas*. Subsurface Memoir of the British Geological Survey, Nottingham, 130 pp.

**Larsen, P-H.** (1988) Relay structures in a Lower Permian basement-involved extension system, East Greenland. *Journal of Structural Geology*, **10**, 3-8.

**Leclair, S.F.** and **Bridge, J.S.** (2001) Quantitative interpretation of sedimentary structures formed by river dunes. *Journal of Sedimentary Research*, **71**, No. 5, 713-716.

**Leclair, S.F.** (2011) Interpreting fluvial hydromorphology from the rock record: Large-river peak flows leave no clear signature. In: *From River To Rock Record: The Preservation Of Fluvial Sediments And Their Subsequent Interpretation* (Eds S.K. Davidson; S. Leleu and C.P. North), *SEPM Spec. Publ.*, **97**, 113-123.

**Leeder, M.R.** (1982) Upper Palaeozoic basins of the British Isles-Caledonide inheritance versus Hercynian plate margin processes. *Journal of the Geological Society*, **139**, 479-491.

**Leeder, M.R.** (1988) Recent developments in Carboniferous geology: a critical review with implications for the British Isles and N.W. Europe. *Proceedings of the Geologists' Association*, **99**, 73-100.

**Linton, D.L.** (1955) The Problem of Tors. *The Geographical Journal*, **121** (4), 470-481.

**Martinsen, O.J.** (1990) *Interaction between eustasy, tectonics and sedimentation with particular reference to the Namurian Elc-H2c of the Craven-Askrigg area, northern England*. Unpublished Doctoral Sc. thesis, University of Bergen, Norway.

**Martinsen, O.J.** (1993) Namurian (late Carboniferous) depositional systems of the Craven-Askrigg area, northern England: implications for sequence-stratigraphic models. In: *Sequence Stratigraphy and Facies Associations* (Eds H.W. Posamentier; C.P. Summerhayes; B.U. Haq and G.P. Allen), *Int. Assoc. Sedimentol. Spec. Publ.,* **18**, 247-281.

**Martinsen, O.J., Collinson, J.D.** and **Holdsworth, B.K.** (1995) Millstone Grit cyclicity revisited, II: sequence stratigraphy and sedimentary responses to changes of relative sea-level. In: *Sedimentary Facies Analysis: A Tribute to the Research and Teaching of Harold G. Reading* (Ed. G. Plint), *Int. Assoc. Sedimentol. Spec. Publ.,* **22**, 305-327.

**McCabe, P.J.** (1977) Deep distributary channels and giant bedforms in the Upper Carboniferous of the Central Pennines, northern England. *Sedimentary Geology*, **24**, 271-290.

**Miall, A.D.** (1976) Facies Models 4. Deltas. *Geoscience Canada*, **3**, 215-227.

**Miall, A.D.** (1985) Architectural-element analysis: a new method of facies analysis applied to fluvial deposits. *Earth-Science Reviews*, **22**, 261-308.

**Miall, A.D.** (2010a) Alluvial Deposits. In: *Facies Models 4* (Eds N.P. James and R.W. Dalrymple), *Geological Association of Canada*, 105-137.

**Miall, A.D.** (2010b) *The Geology of Fluvial Deposits: Sedimentary Facies, Basin Analysis and Petroleum Geology*. Fourth Edition. Springer, 582 pp.

**Miall, A.D.** (2014) *Fluvial Depositional Systems*. Springer, Switzerland, 316 pp.

**Mumpy, A.J., Jol, H.M., Kean, W.F.** and **Isbell, J.L.** (2007) Architecture and sedimentology of an active braid bar in the Wisconsin River based on 3-D ground penetrating radar. In: *Stratigraphic Analysis Using GPR* (Eds G.S. Barker and H.M. Jol), *Geological Society of America Special Paper,* **432**, 111-131

**Olsen, T., Steel, R., Hogseth, K., Skar, T.** and **Roe, S.** (1995) Sequential architecture in a fluvial succession: sequence stratigraphy in the Upper Cretaceous Mesaverde Group, Price Canyon, Utah: *Journal of Sedimentary Research*, **65**, 265-280.

**Palmer, J.** and **Radley, J.** (1961) Gritstone tors of the English Pennines. In: *Zeitsschrift Für Geo-morphologie*, **5**, 37-52.

**Peacock, D.C.P.** and **Sanderson, D.J.** (1994) Geometry and Development of Relay Ramps in Normal Fault Systems. *American Association of Petroleum Geologists Bulletin*, **78**, 147-165.

**Phillips, J.** (1836) *Illustrations of the Geology' of Yorkshire, Part 11. The Mountain Limestone District*. Murray, London, 253 pp.

**Ramsbottom, W.H.C.** (1977) Major cycles of transgression and regression (Mesothems) in the Namurian. *Proceedings of the Yorkshire Geological Society*, **41**, 261-291.

**Ramsbottom, W.H.C.** (1979) Rates of transgression and regression in the Carboniferous of NW Europe. *Journal of the Geological Society*, **136**, 147-153.

**Reesink, A.J.H.** and **Bridge, J.S.** (2007) Influence of superimposed bedforms and flow unsteadiness on formation of cross strata in dunes and unit bars. *Sedimentary Geology*, **202**, 281-296.

**Reesink, A.J.H.** and **Bridge, J.S.** (2009) Influence of bedform superimposition and flow unsteadiness on the formation of cross strata in dunes and unit bars - Part 2, further experiments. *Sedimentary Geology*, **222**, 274-300.

**Reesink, A.J.H., Ashworth, P.J., Sambrook Smith, G.H., Best, J.L., Parsons, D.R., Amsler, M.L., Hardy, R.J., Lane, S.N., Nicholas, A.P., Orfeo, O., Sandbach, S.D., Simpson, C.J.** and **Szupiany, R.N.** (2014) Scales and causes of heterogeneity in bars in a large multi-channel river: Río Paraná, Argentina. *Sedimentology,* **61**, 1055-1085.

**Reid, C.T.** (1996) *The Alportian and Kinderscoutian (Namurian) of North Yorkshire: the sedimentary response to eustatic variation*. Unpublished Doctoral thesis, University of Keele.

**Rubin, D.M.** and **Carter, C.L.** (2006) *Bedforms and Cross-Bedding in Animation*. SEPM, Atlas Series, 2, DVD.

**Singh, A.** and **Bhardwaj, B.D.** (1991) Fluvial facies model of the Ganga River sediments, India. *Sedimentary Geology*, **72**, 135-146.

**Skelly, R.L., Bristow, C.S.** and **Ethridge, F.G.** (2003) Architecture of channel-belt deposits in an aggrading shallow sandbed braided river: the lower Niobrara River, northeast Nebraska. *Sedimentary Geology*, **158**, 249-270.

**Smith, N.D.** (1972) Some Sedimentological Aspects of Planar Cross-Stratification in a Sandy Braided River. *Journal of Sedimentary Petrology*, **42**, 624-634.

**Stone, P., Millward, D., Young, B., Merritt, J.W., Clarke, S.M., McCormac, M.** and **Lawrence, D.J.D.** (2010) *British Regional Geology: Northern England*, 5th edn, British Geological Survey, Nottingham, 294 pp.

**Sundborg, A.** (1956) The River Klarälven: A Study of Fluvial Processes. *Geografiska Annaler*, **38**, No. 2, 125-237.

**Thompson, A.T.** (1957) *The structure and stratigraphy of Nidderdale between Lofthouse and Dacre*. Unpublished, Doctoral thesis, Durham University. Available at Durham E-Theses Online: http://etheses.dur.ac.uk/ 722/.

**Walker, C.T.** (1952) *Stratigraphical directional studies in the Kinderscout Grits of Wharfedale and adjacent areas*. Unpublished Doctoral thesis, University of Leeds.

**Walker, R.G.** (1966) Shale Grit and Grindslow Shales: Transition from Turbidite to Shallow Water Sediments in the Upper Carboniferous of Northern England. *Journal of Sedimentary Petrology*, **36**, 90-114.

**Waters, C.N., Chisholm, J.I., Benfield, A.C.** and **O'Beirne, A.M.** (2008) Regional Evolution of a Fluvio deltaic Cyclic Succession in the Marsdenian (late Namurian Stage, Pennsylvanian) of the Central Pennine Basin, UK. *Proceedings of the Yorkshire Geological Society*, **57**, 1-28.

**Waters, C.N.** (2011a) Definitions of chronostratigraphic subdivisions: geochronology and event stratigraphy. In: *A Revised Correlation of Carboniferous Rocks in the British Isles* (Ed. C.N. Waters), *Geological Society Special Report*, No. **26**, 3-10.

**Waters, C.N., Jones, N.S., Collinson, J.D.** and **Cleal, C.J.** (2011b) Craven Basin and southern Pennines. In: *A Revised Correlation of Carboniferous Rocks in the British Isles* (Ed. C.N. Waters), *Geological Society Special Report*, No. **26**, 74-81.

**Waters, C.N., Dean, M.T., Jones, N.S.** and **Somerville, I.D.** (2011c) Cumbria and the northern Pennines. In: *A Revised Correlation of Carboniferous Rocks in the British Isles* (Ed. C.N. Waters), *Geological Society Special Report*, No. **26**, 82-88.

**Waters, C.N.** and **Condon, D.J.** (2012) Nature and timing of Late Mississippian to Mid-Pennsylvanian glacio-eustatic sea-level changes of the Pennine Basin, UK. *Journal of the Geological Society, London*, **169**, 37-51.

**Wilson, A.A.** (1957) *Geology of the country between Masham and Great Whernside*. Unpublished Doctoral thesis, Durham University. Available at Durham E-Theses Online: http://etheses.dur.ac.uk/1363/.

**Wilson, A.A.** and **Thompson, A.T.** (1965) The Carboniferous section in the Kirkby Malzeard area, Yorkshire. *Proceedings of the Yorkshire Geological Society*, **35**, Part 2, 203-227.

**Wilson, A.A.** (2006) The Carboniferous Rocks of upper Nidderdale (Field excursion). In: *Yorkshire rocks and Landscape. A Field Guide*, *3*rd edn, (Eds C. Scrutton and J.H. Powell). *Yorkshire Geological Society*, 224 pp.

## TABLE AND FIGURE CAPTIONS

**Table 1.** Summary description and interpretation of the sub-facies characteristic types associated with the Lower Brimham Grit, as exposed at Brimham Rocks. Primary facies codes adapted from Miall, 2010a, 2010b, 2014; Colombera *et al.*, 2012a, 2012b; 2013 are also included (see Fig. 5 for application of colour-coded scheme).

**Fig. 1.** Typical Bashkirian (Kinderscoutian Regional Substage, *ca* 321 to 320 Ma) outcrops observed at Brimham Rocks showing Location 1 (Coordinate N54° 4' 49.2" – W1° 41' 7.5"); views towards 130° (A) and 321° (B). Outcrops consist primarily of pebbly quartzo-feldspathic (subarkose) sandstone of the Lower Brimham Grit (Namurian Millstone Grit). Lettering and arrows indicate the relative position and view of architectural panel examples (see Figs 7 and 8).

**Fig. 2.** Geological overview map of the British Isles and Ireland (A); Brimham Rocks study area is shown centred on coordinate N54˚ 4' 50" – W1˚ 40' 50". (B) Detailed geological map highlighting the geology associated with the study and adjacent areas; location names are also shown. (C) Google

Earth image aerial view of Brimham Rocks showing study localities 1 and 2 that are explicitly mentioned in the text (modified in part after Kirby *et al.,* 2000; Waters *et al.,* 2011b, 2011c; Google Earth, 2013).

**Fig. 3.** Summary of Carboniferous chronostratigraphy (A), biostratigraphy (B) and lithostratigraphy (C) associated with the Lower Brimham Grit; Kinderscoutian interval is shaded green (modified in part after Dunham & Wilson, 1985; British Geological Survey, 2008; Davydov *et al.*, 2010; Waters, 2011a; Waters *et al.*, 2011b; Waters and Condon, 2012).

**Fig. 4.** Composite of key features and locations: (A) Dinantian (359.2 to 330 Ma) and Mid Namurian (*ca* 325 to 320 Ma) palaeogeographic map of the Central Province of northern England (CP) relating to the Variscan Orogeny and main depositional regimes, respectively; inset depicts CP relative to the UK. (B) Variscan fault structures which influenced Carboniferous basin formation. (C) Diagram depicting envisaged scenario of a fault relay zone influencing palaeocurrents around Brimham Rocks. Figures modified in part after: (A) Collinson (1988), Cope *et al.*, (1992), Corfield *et al.* (1996), Hunter (2001), Guion *et al.* (2010); (B) Kirby *et al.* (2000).

**Fig. 5.** Composite figure depicting: (A) Colour-coded primary facies (adapted from Miall, 2010a, 2010b, 2014; Colombera *et al.*, 2012a, 2012b; 2013) and sub-facies classification scheme (specifically for the Lower Brimham Grit). (B) Symbol legend. (C) Cartoon showing bar and dune terminology relating to measurement orientations referred to in the text. Sub-facies classification scheme and legend relate to all figures depicting log profiles and architectural panels with summary sub-facies scheme provided for ease of reference. Colour-coding adopted to facilitate recognition and association comparisons between sub-facies and/or bounding surfaces, for example. See Table 1 for explanation of sub-facies codes.

**Fig. 6.** Annotated examples of Lower Brimham Grit sub-facies and associations observed at Brimham Rocks. (A) *Sl-hss <1.0 m*; cross-cutting tabular cosets recording downstream-accretion. (B) *Stlx >3.0 m*; large-scale trough cross-bedding representing migration of a sandy bedform. (C) *Sl-hpx >2.0 m*; very-large-scale planar cross-bedding 'alternate bar'. (D) *Sl-hhs <1.0 m*; cosets of planar horizontal sets recording downstream migration and net aggradation. (E) *Spl/b*; laminated beds, grain-size distribution and lack of mica are typical of upper plane bed flow regime deposition. (F) *Spb >15%*; pebble-rich set with poorly defined planar cross-bedding. (G) *Sfp*; preserved *Calamites* remnant implies rapid deposition which facilitated fossil preservation. (H) *Ssd;* soft-sediment deformation, loss of grain stability within unconsolidated water laden sediments. See Table 1 for explanation of sub-facies codes.

**Fig. 7.** Aerial view of Locations 1 and 2 (Fig. 2C) overlain with Ordnance Survey grid and 5 m contour lines with Locations 1 and 2 bounded by yellow outlines. Orange lettering ('A' to 'D') and red arrows indicate the position and view of architectural panel examples (Figs 1 and 8). Red lettering ('E' to 'Q') indicates the position of log profiles (Fig. 9). Yellow lettering ('R' to 'W') indicates the position of architectural element examples (Fig. 10). Grid, contour lines and image modified from Edina Digimap (2013) and Google Earth (2013), respectively.

**Fig. 8.** Four detailed architectural panels (A to D) depicting the vertical and lateral extent of component lithofacies and associated architectural elements from Location 1 (Figs 1, 2C and 7). The juxtaposition of lithofacies morphologies implies that their deposition probably was influenced by complex palaeocurrents associated with two distinct palaeocurrent regimes. South/south-easterly palaeocurrents dominated the lower downstream-accretion architectural element, whereas westerly palaeocurrents influenced the upper channel architectural elements (see Fig. 9 for related log profiles G to I and architectural element scheme).

**Fig. 9.** Thirteen detailed representative sedimentary graphic log profiles (E to Q) for the Lower Brimham Grit succession (Locations 1 and 2; see Figs 2C and 7). Log profiles show sub-facies and architectural element associations with correlated arrows depicting mean palaeocurrent azimuth-dips (channel data relate to channel bounding surface-dips). Colour-coding applies to all figures and is adopted to facilitate: (i) recognition and comparison between associations of sub-facies and architectural elements; and (ii) differentiation of palaeocurrent data between, for example, foreset, set and coset azimuth-dips and channel bounding surface-dips.

**Fig. 10.** Six detailed 2D panels (R to W) depicting characteristic architectural element types for the Lower Brimham Grit (see Fig. 7 for element locations). Examples presented are judged to be representative illustrations of the recognized element types. Panels also include summary rose diagrams illustrating mean palaeocurrent azimuth-dips.

**Fig. 11.** Five statistical graphs comparing primary facies-unit types associated with sections of modern and ancient braided fluvial systems: (A) Brahmaputra (Jamuna; Bristow, 1993). (B) Gash (Abdullatif, 1989). (C) Ganges (Singh & Bhardwaj, 1991). (D) Rio Vero Formation (Jones *et al*., 2001). (E) Brimham Rocks (this study). Pie charts depict percentage of facies-unit types present with bar charts depicting average facies-unit type thickness (left column) and percentage of total facies-unit type transitions (right column). All data, including primary facies-unit types and description scheme are adapted from the Fluvial Architecture Knowledge Transfer System (FAKTS; Colombera *et al*., 2012a, 2012b, 2013). Three bar charts depicting relationships between combined thickness (F), percentage of total combined thickness (G) and percentage of total number of elements (H) for each architectural element associated with log profiles E to Q. Composite sedimentary graphic log profile (I) assembled from a précis of log profile P, J and E displaying a 32 m vertical section of the Lower Brimham Grit (Locations 1 and 2, see Figs 7, 9 and 13).

**Fig. 12.** Expanded view of Fig. 1B showing a section of the main outcrop at Location 1 (Figs 2C and 7). The image is annotated with a hierarchy of three relatively shallow and broad main channel elements identified within the outcrop; the middle channel element incises *ca* 4 m into underlying strata.

**Fig. 13.** Two pseudo-3D box panels displaying spatial relationships between log profiles and associated architectural elements, as observed at Locations 1 and 2. Log profiles F to Q (Figs 7 and 9) are depicted positioned with regard to their latitude and longitude coordinates and stratigraphic level, log profile E is not included. Blue shaded areas show the inferred position of stacked and laterally migrating channel elements.

**Fig. 14.** Schematic diagram depicting predicted channel and barform relationships based on observations relating to log profile Q (N54˚ 4' 37.9" – W1˚ 41' 1.5") and O (N54˚ 4' 39.5" – W1˚ 41' 3.7"), see Figs 7, 9, 13 and 15; Location 2. Mean palaeocurrent data and sedimentary facies and architectural element relationships demonstrate an episode of channel incision and thalweg migration.

**Fig. 15.** Schematic block diagram representing a detailed hypothetical facies depositional model portraying scenarios to account for the distinct variation in the facies, architectural element arrangements and palaeocurrent data between the successions studied at Locations 1 and 2. See text for explanation.

**TABLE 1.**

| Facies<br><br>Sub-facies | Colour | Lithology | Contacts | Primary (1) and secondary (2)<br><br>sedimentary structures | Bounding<br><br>surface | Interpretation |
|---|---|---|---|---|---|---|
| St<br><br>Stsx <1.5 m | Light beige/grey | Medium-grained to granular sandstone with <10% small pebble content, low to high sphericity, angular to sub-angular and moderate to well-sorted grains; predominantly quartz with some feldspar (Orthoclase) | Sharp, horizontal to sub-horizontal and evidence of erosion between beds | (1) Small-scale cross-cutting trough cross-bedding <1.5 m trough width; pebble inclusions<br><br>(2) Sets and cosets | First, Second and Third-order | Aggradation with net migration of relatively small sinuous-crested dunes (3D mesoform); downstream-accretion (DA macroform); set and coset boundaries form First and Second-order bounding surfaces respectively; sub-horizontal erosional contacts form Third-order bounding surfaces |
| St<br><br>Stmx 1.5 to 3.0 m | Light beige/grey | Medium-grained to granular sandstone with <10% small pebble content; highly spherical, rounded to sub-rounded and moderately to well-sorted grains; predominantly quartz | Sharp, sub-horizontal and evidence of erosion between beds | (1) Medium-scale cross-cutting trough cross-bedding, 1.5 to 3.0 m long shallow trough width<br><br>(2) Reactivation surface | First and Third-order | Aggradation with net migration of relatively small- to medium sinuous-crested dunes (3D mesoform); downstream-accretion (DA macroform); reactivation surface and sub-horizontal contact form First and Third-order bounding surfaces, respectively |
| St<br><br>Stlx >3.0 m | Light beige/grey | Medium-grained to granular sandstone with <10% small pebble content; highly spherical, rounded and well-sorted grains; predominantly quartz | Sharp, horizontal erosional and/or gradual contact between beds | (1) Large-scale trough cross-bedding >3.0 m long shallow trough width | - | Aggradation with net migration of relatively large sinuous-crested dunes (3D mesoform); migration of sandy bedform (SB mesoform) and channel fill component |
| Sp<br><br>Sl-hpx <2.0 m | Light beige/grey | Medium-grained to granular sandstone; low sphericity, sub-angular and poorly sorted grains; predominantly quartz with some feldspar (Orthoclase) | Sharp, horizontal erosional and/or gradual contact between beds | (1) Low to high-angle-inclined foresets forming small to large-scale planar (tabular) cross-bedding<br><br>(2) Reactivation surface; suspension/<br><br>avalanche deposit | First-order | Aggradation with net migration of small to large-scale straight crested dunes (2D mesoform); set thickness provides an indication of overall dune height, channel flow depth and amount of sediment input; migration of sandy bedform (SB mesoform) and channel fill component; suspension deposits interbedded with avalanche strata represent fining-up foreset succession and reactivation surfaces form First-order bounding surfaces |
| Sp<br><br>Sl-hpx >2.0 m | Light beige | Coarse-grained to granular sandstone with <10% small pebble content, highly spherical, sub-rounded and moderately sorted grains; predominantly quartz with some feldspar (Orthoclase) | Sharp, sub-horizontal contact with underlying bed | (1) Low to high-angle-inclined foresets forming very large-scale planar cross-bedding<br><br>(2) Reactivation surface; suspension/<br><br>avalanche deposit | First-order | Aggradation with net migration of relatively substantial planar straight crested bedforms (3D macroform) within a comparatively large and deep fluvial channel; possible migrating “alternate bar” (macroform), oblique downstream-accretion (DA macroform); suspension deposits interbedded with avalanche strata represent fining-up foreset succession and reactivation surfaces form First-order bounding surface. |
| Sl<br><br>Sl-hss <1.0 m | Light beige | Medium- to very coarse-grained sandstone with highly spherical, rounded- to sub-rounded and well sorted grains; predominantly quartz | Boundaries may show sharp sub-horizontal contact and evidence of erosion between sets | (1) Low to high-angle-inclined foresets forming >1 sub-horizontal set; variable set thickness of <1.0 m thick<br><br>(2) Reactivation surface; suspension/<br><br>avalanche deposit | First and Third-order | Aggradation with net migration of relatively small to medium-scale straight or sinuous-crested dunes (2D or 3D mesoform, respectively); set thickness provides an indication of overall dune height, flow depth along channel, or bar front/crest, and amount of sediment input; downstream-accretion (DA macroform); suspension deposits interbedded with avalanche strata represent fining-up foreset succession; set boundaries, reactivation surfaces and sub-horizontal contacts form First-order and Third-order bounding surfaces, respectively. |
| Sl<br><br>Sl-hss-of <0.2 m | Light beige | Medium to very coarse-grained sandstone with highly spherical, rounded and well-sorted grains; predominantly quartz | Sharp, sub-horizontal contact with evidence of erosion between sets | (1) Low to high-angle-inclined foresets forming >1 sub-horizontal set with oblique cross-bedding foresets; variable set thickness of <0.2 m thick | First and Third-order | Aggradation with net lateral migration of relatively small-scale sinuous-crested dunes (3D mesoform); lateral-accretion (LA mesoform) migration; set boundaries and sub- horizontal contacts form First-order and Third-order bounding surfaces, respectively. |
| Sh<br><br>Sl-hhs <1.0 m | Light beige | Medium to very coarse-grained sandstone with highly spherical, rounded to sub-rounded and well-sorted grains; predominantly quartz | Sharp, horizontal contact with evidence of erosion between sets | (1) Low to high-angle-inclined foresets forming >1 horizontal set; variable set thickness of <1.0 m thick<br><br>(2) Reactivation | First-order | Migration with net aggradation of relatively small to medium-scale straight or sinuous-crested dunes (2D or 3D mesoform, respectively); set thickness provides an indication of overall dune height, channel, or bar top, flow depth and amount of sediment input; migration of sandy bedform (SB mesoform) and channel fill component; suspension deposits interbedded with avalanche strata represent fining-up foreset |

| | | | | | | |
|---|---|---|---|---|---|---|
| | | | | surface; suspension/<br><br>avalanche deposit | | succession; set boundaries and reactivation surfaces form First-order bounding surfaces |
| Sh<br><br>Spl/b | Light beige | Fine- to medium-grained sandstone with highly spherical, well rounded and very well sorted grains; predominantly quartzarenite | Sharp, horizontal, inclined and/or gradual contact which may show evidence of erosion between beds | (1) Planar horizontal laminations 2 to 4 mm thick<br><br>(2) 10 to 30 mm thick horizontal beds | - | Aggradation and net migration with gradual evolution from trough cross-bedding to planar laminations, inferring reduction in channel/water depth and transition to 'upper flow regime flat bed' ('upper plane bed'); migration of sandy bedform (SB mesoform) and channel fill component |
| Gt/p<br><br>Spb >15% | Light beige/grey | Granular sandstone with >15% small pebble content, highly spherical, sub-rounded and poorly sorted grains; predominantly quartz with some feldspar (Orthoclase) | Poorly to well-defined erosional horizontal contact between beds | (1) Poorly defined planar cross-bedding | - | Aggradation and net migration of medium sized straight crested dunes (2D mesoform) with poorly defined foresets and bedding inferring rapid deposition; migration of pebbly bedform (SB mesoform) and channel fill component |
| Gh<br><br>Ss-lp-lag | Light beige/grey | Very coarse-grained to granular sandstone with <10% small pebble content, low sphericity, sub-angular and poorly sorted grains; predominantly quartz with some feldspar (Orthoclase) | Sharp and sub-horizontal contacts with evidence of erosion between beds | (1) Small to large pebble lag deposit along base 20 to 30 mm thick<br><br>(2) Poorly defined trough or planar cross-bedding | - | Possible minor broad channel scour and/or erosional contact facilitated by a flood event with poorly defined foresets inferring rapid deposition; migration of sandy bedform (SB mesoform). |
| Sf<br><br>Sfp | Light beige/grey | Coarse-grained to granular sandstone with highly spherical, sub-rounded and moderately sorted grains; predominantly quartz with some feldspar (Orthoclase) and up to <10% small pebble content | Sharp and horizontal contacts with evidence of erosion between beds | (1) Structureless with fossilised plant remnants, e.g. calamites and lepidodendron | - | Structureless bedform infers rapid deposition of sandy bedform encasing and facilitating preservation of plant remnants. Calamities probably promoted channel bank and/or channel bar stability, whereas lepidodendron are associated with transient peat-forming swamps |
| Sd<br><br>Ssd<br><br>S-<br><br>Ssb | Light beige | Medium-grained to granular sandstone with highly spherical, rounded and well-sorted grains; predominantly quartz with <10% small pebble content | Sharp and horizontal contacts with evidence of erosion between beds | (1) Planar cross-bedding<br><br>(2) Flame structures | - | Aggradation and net migration of sandy bedform through rapid deposition inhibiting formation of internal sedimentary structures (Ssb), or facilitating total/partial loss of sedimentary structures (Ssd) through liquefaction; migration of sandy bedform (SB mesoform) and channel fill component |

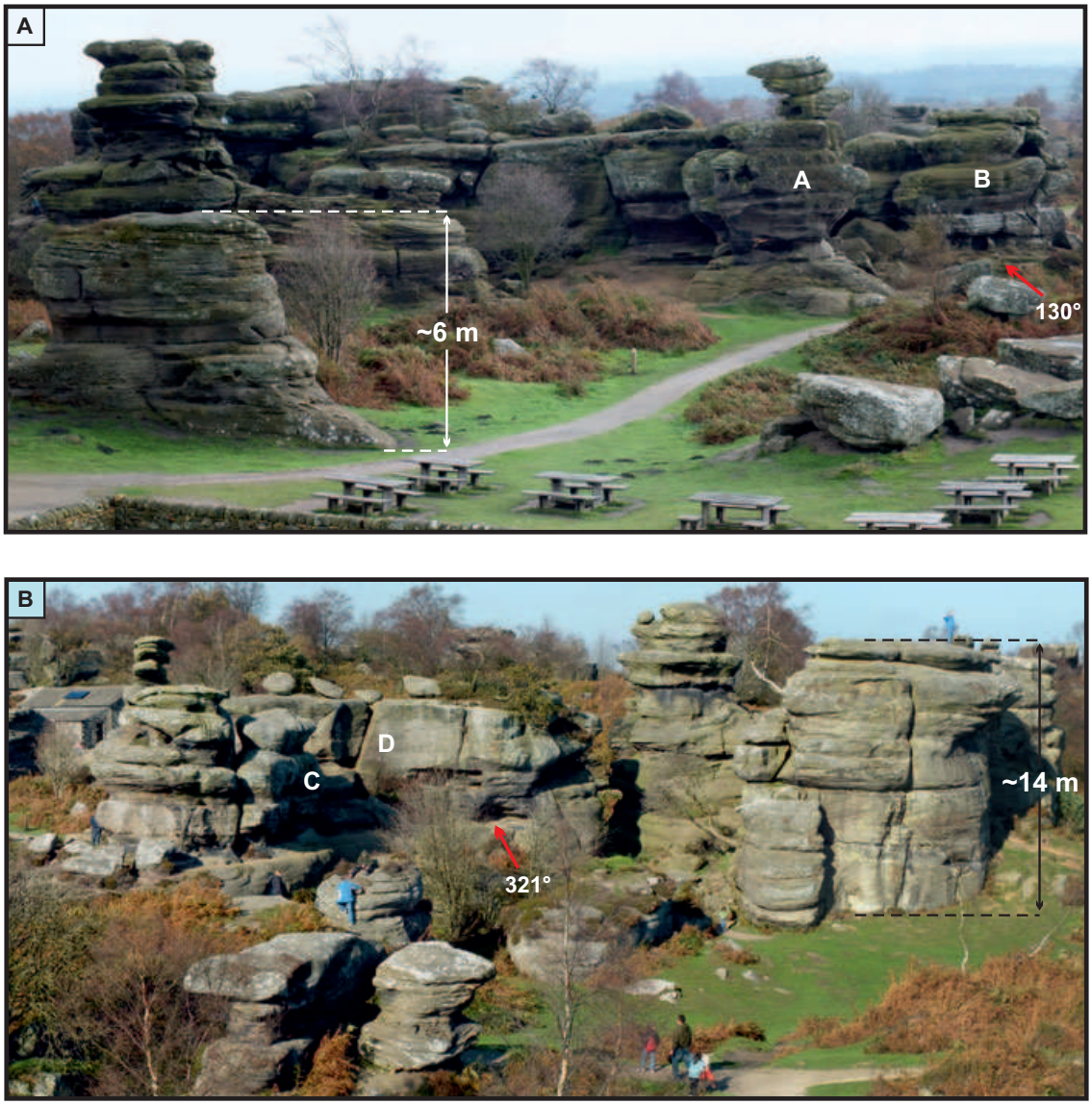


**Fig. 1**

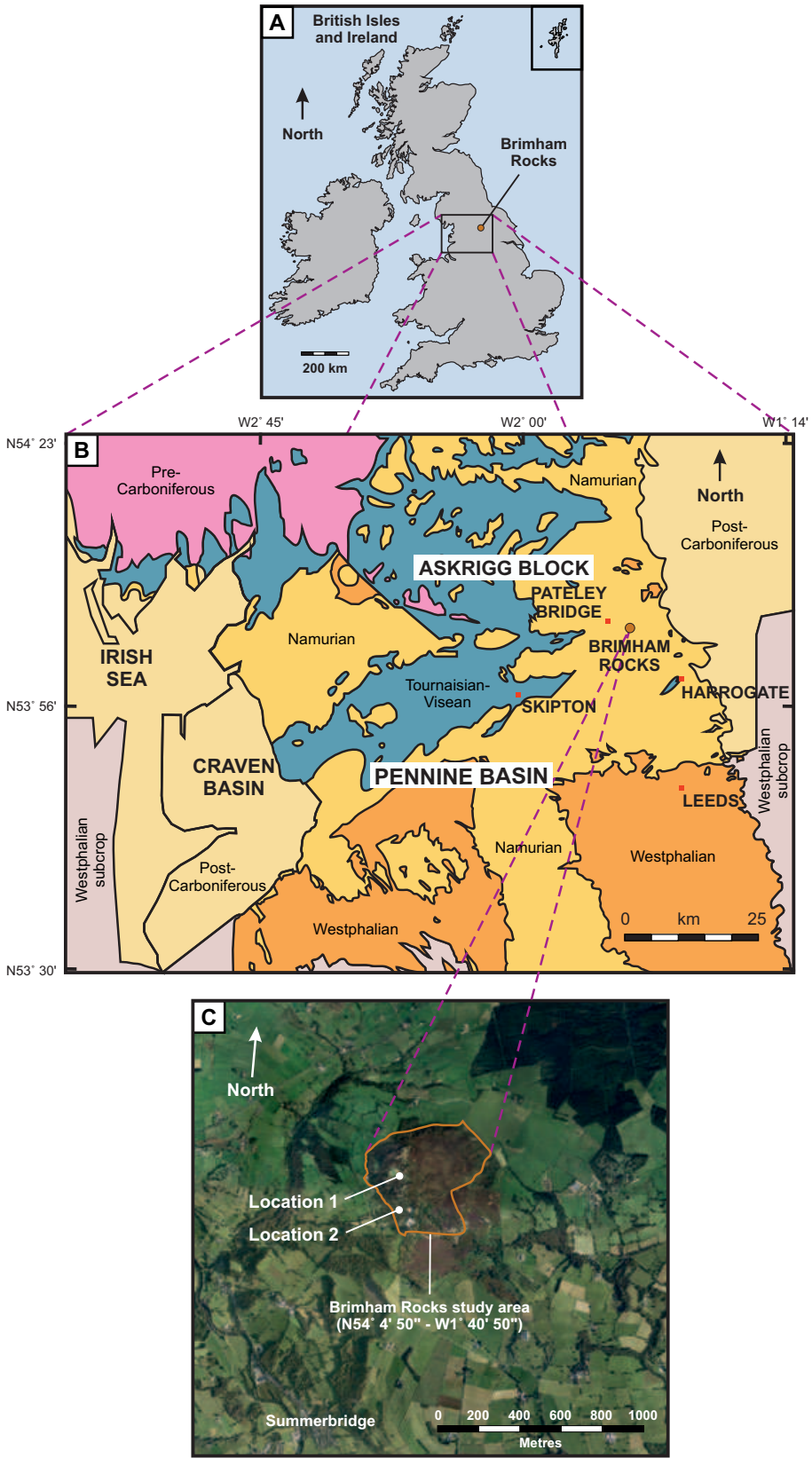


**Fig. 2**

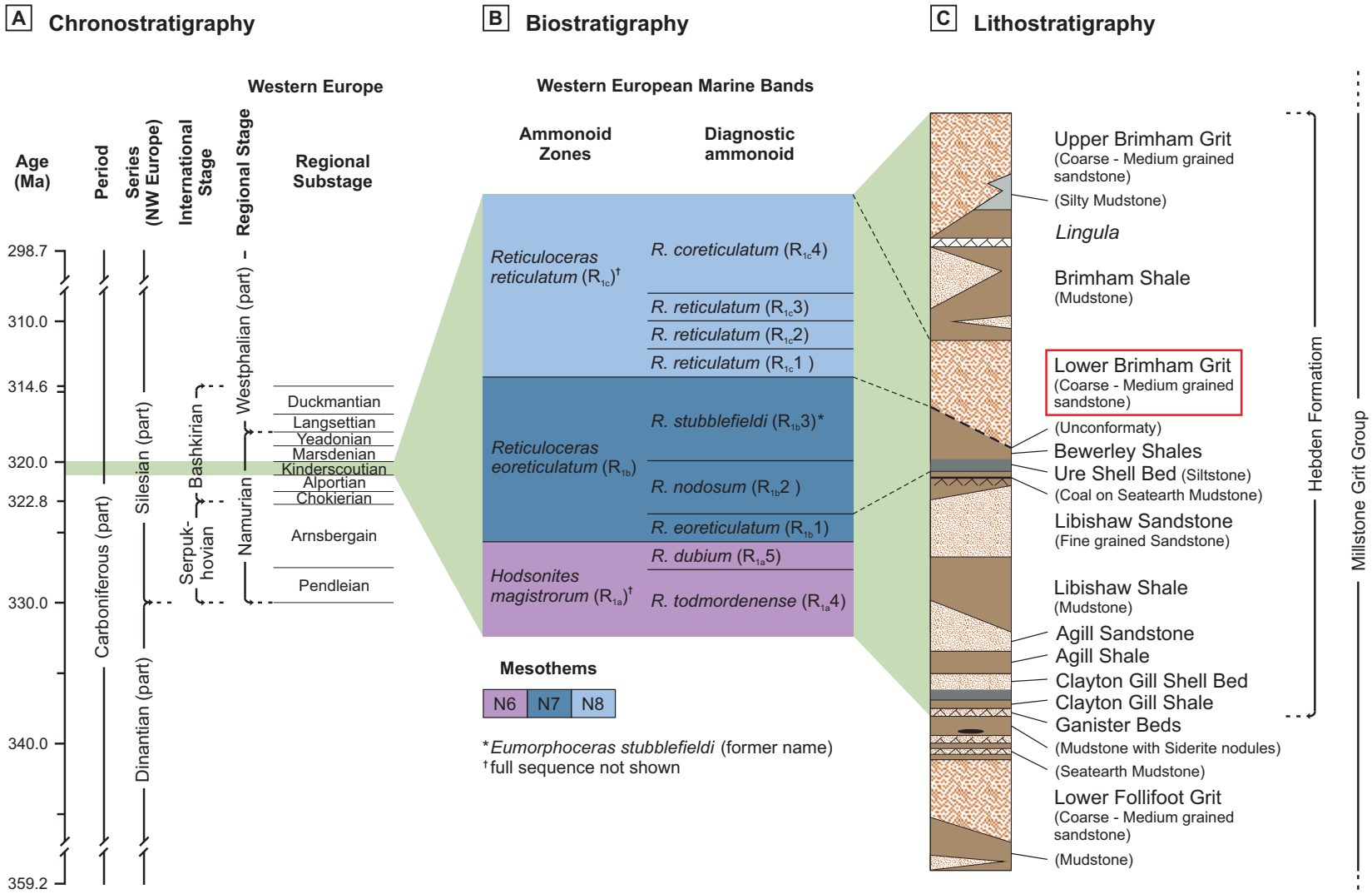


**Fig. 3**

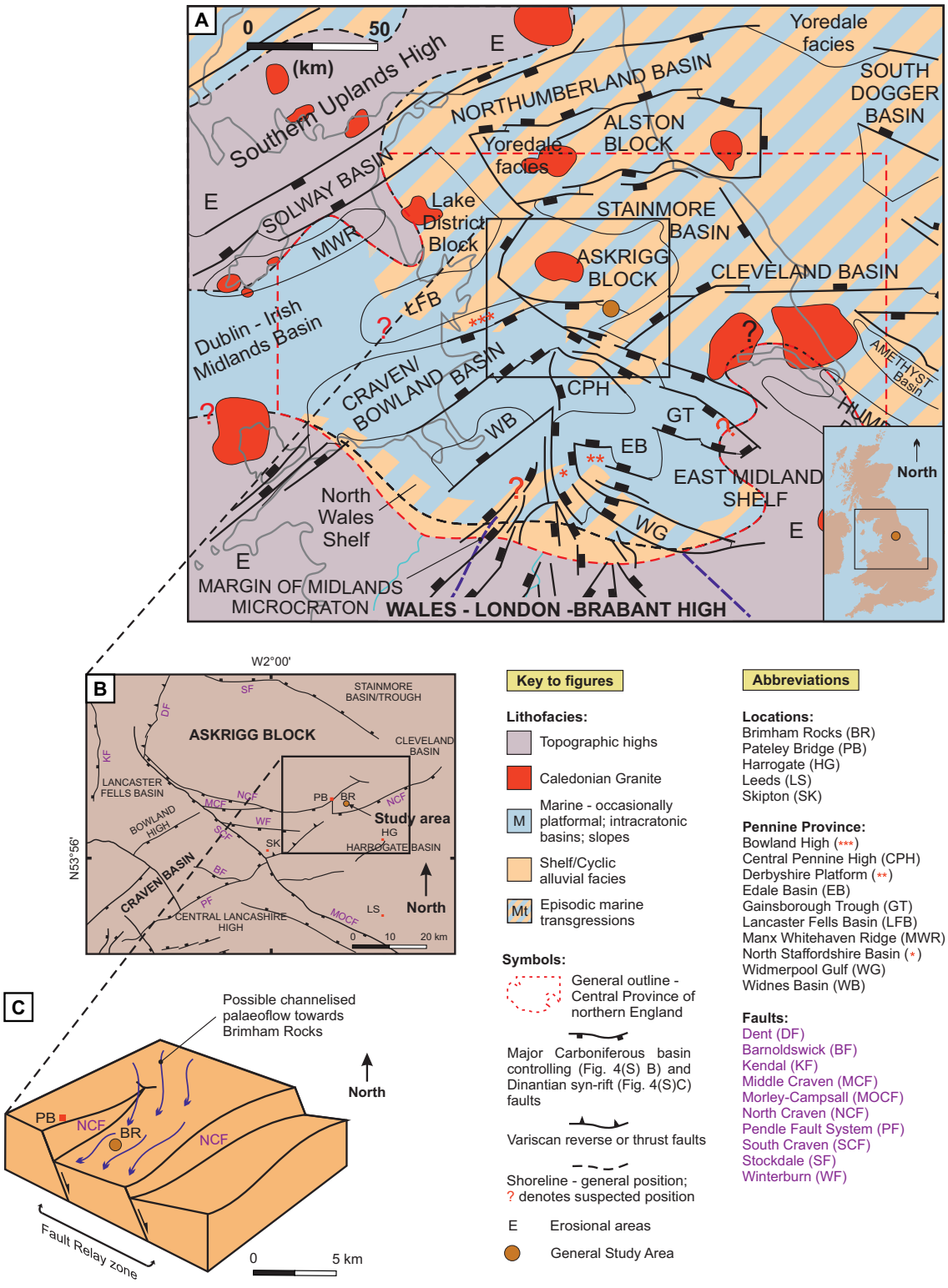


**Fig. 4**

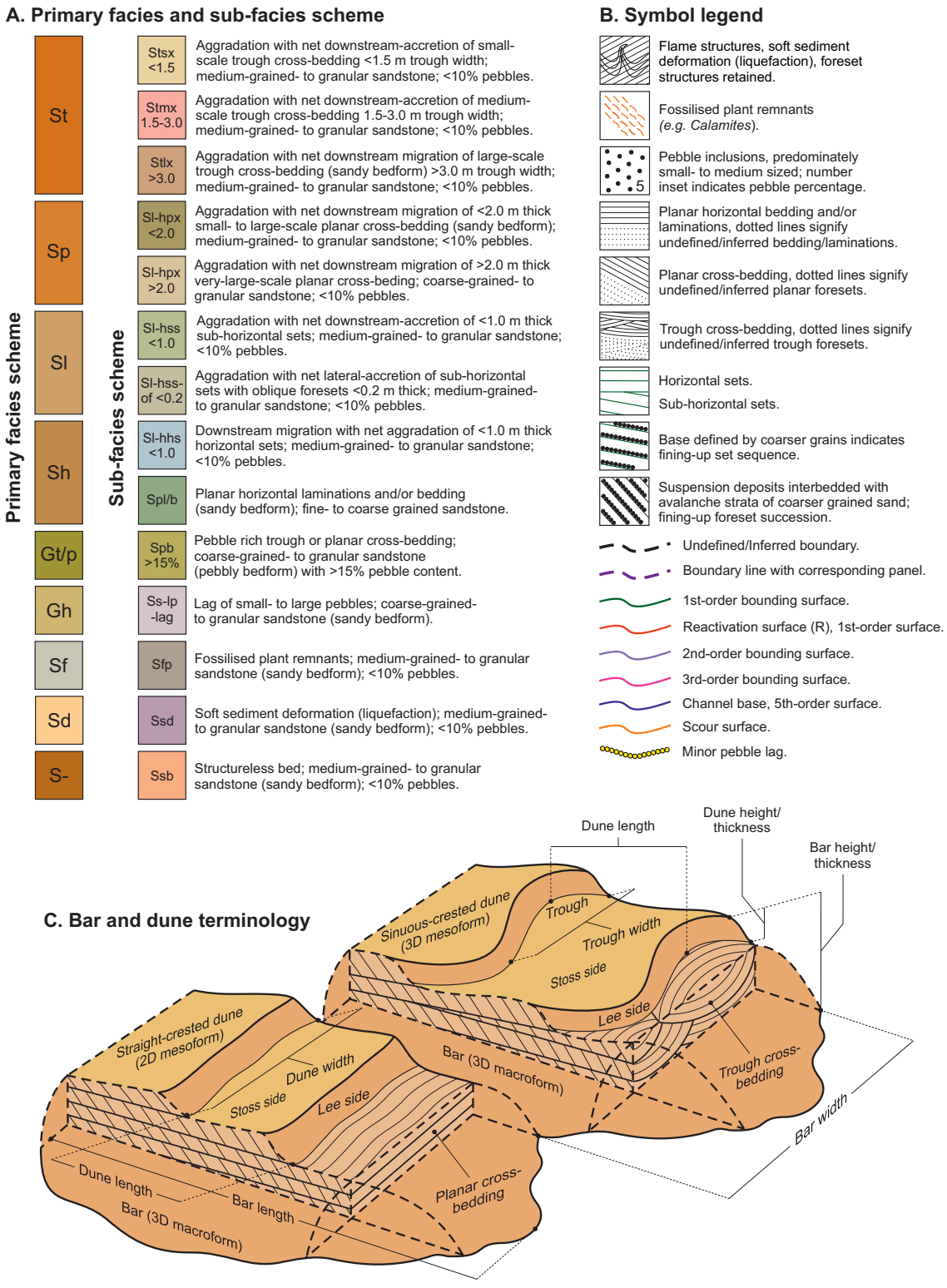


**Fig. 5**

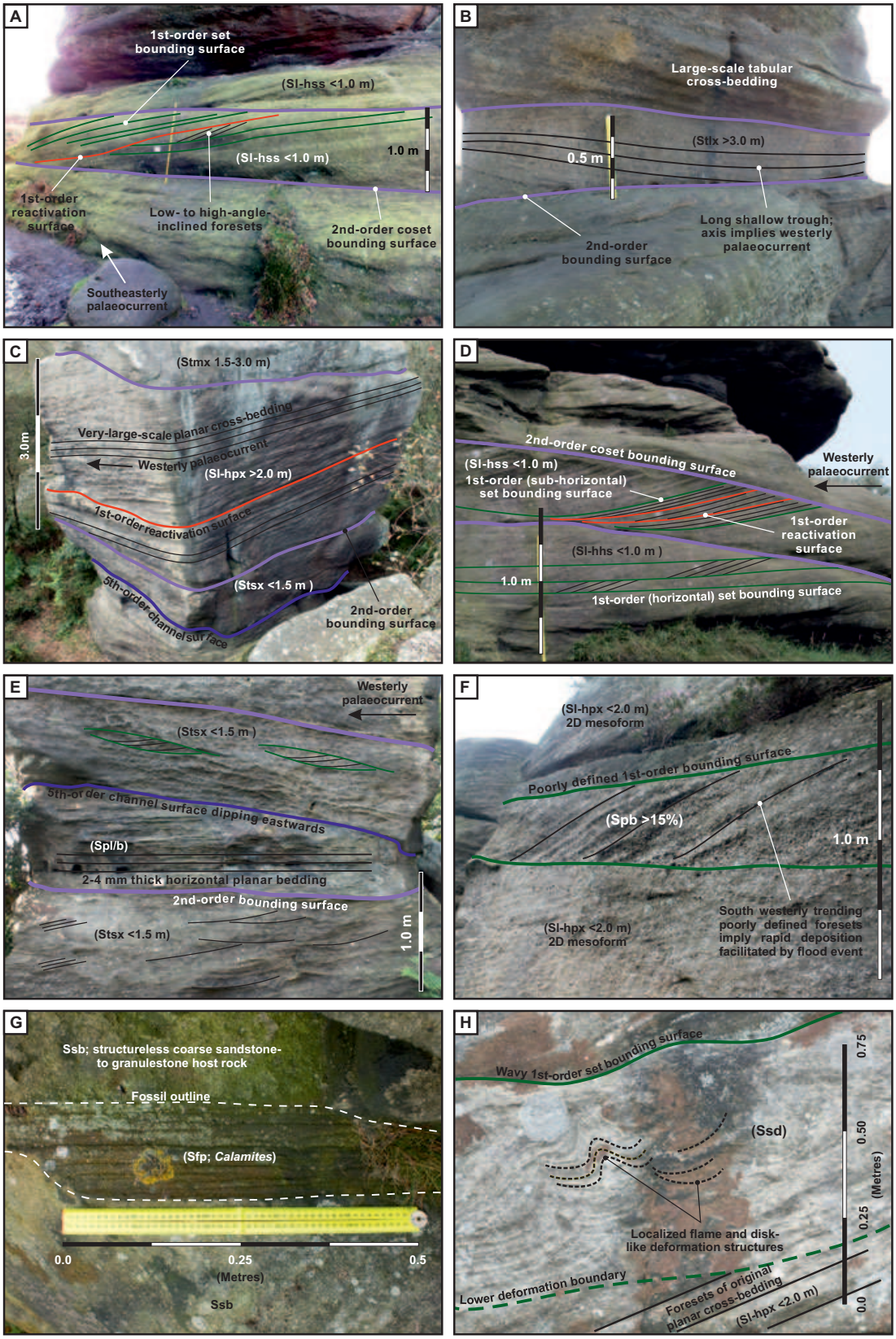


**Fig. 6**

Fig. 7

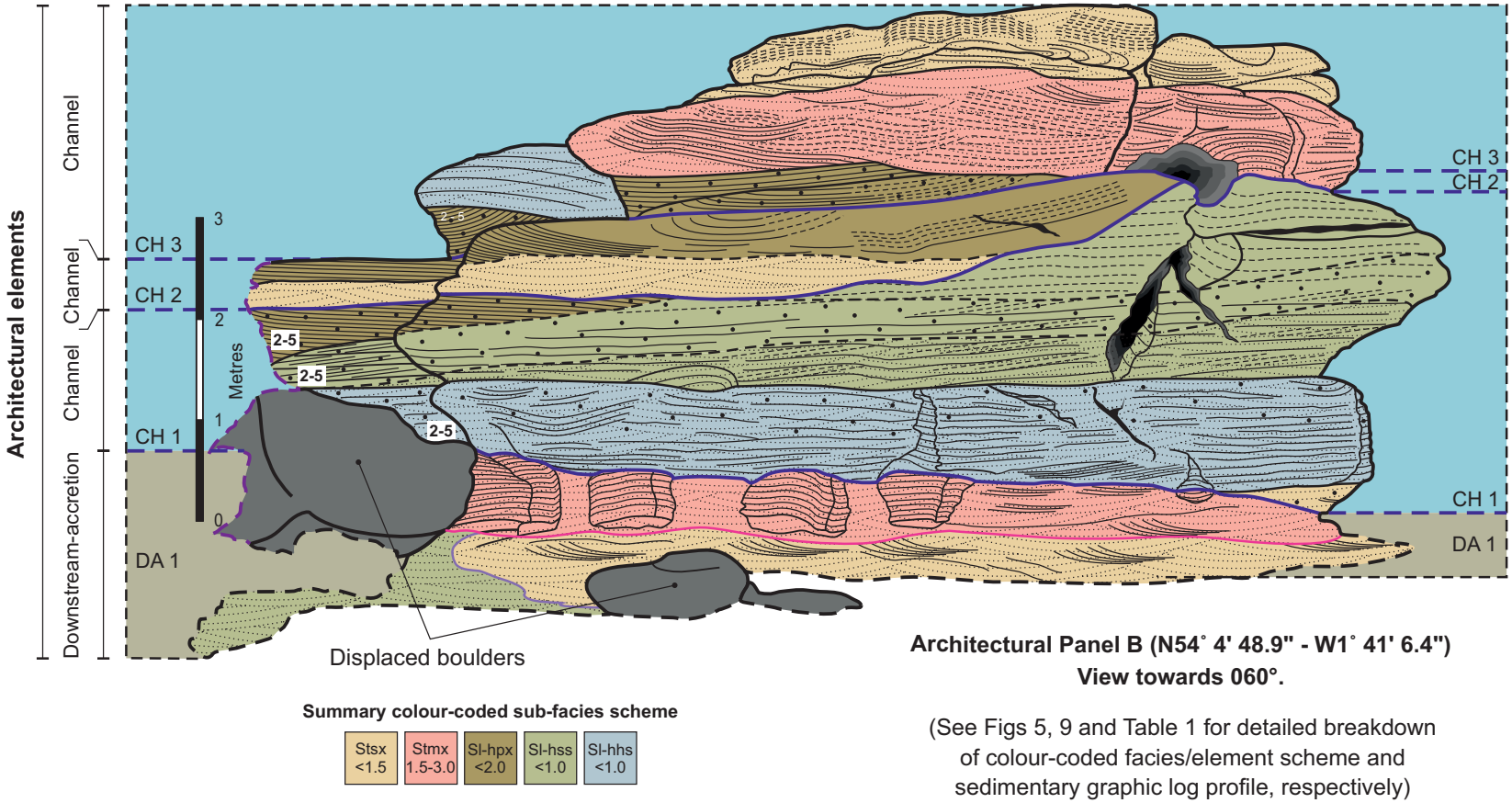


**Architectural Panel B (N54˚ 4' 48.9" - W1˚ 41' 6.4")**
**View towards 060°.**

(See Figs 5, 9 and Table 1 for detailed breakdown of colour-coded facies/element scheme and sedimentary graphic log profile, respectively)

**Fig. 8 Continued**

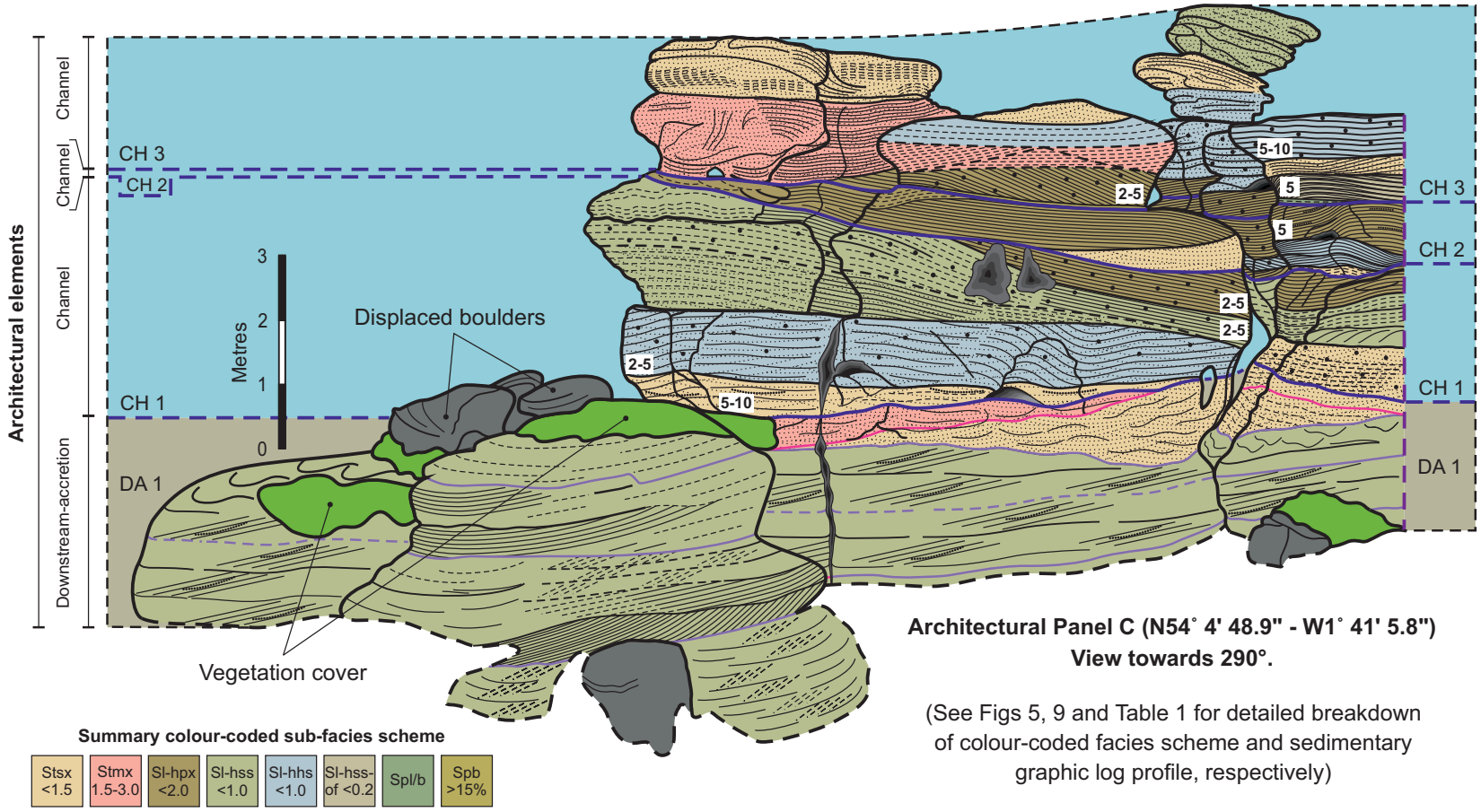


**Architectural Panel C (N54˚ 4' 48.9" - W1˚ 41' 5.8") View towards 290°.**

(See Figs 5, 9 and Table 1 for detailed breakdown of colour-coded facies scheme and sedimentary graphic log profile, respectively)

**Fig. 8 Continued**

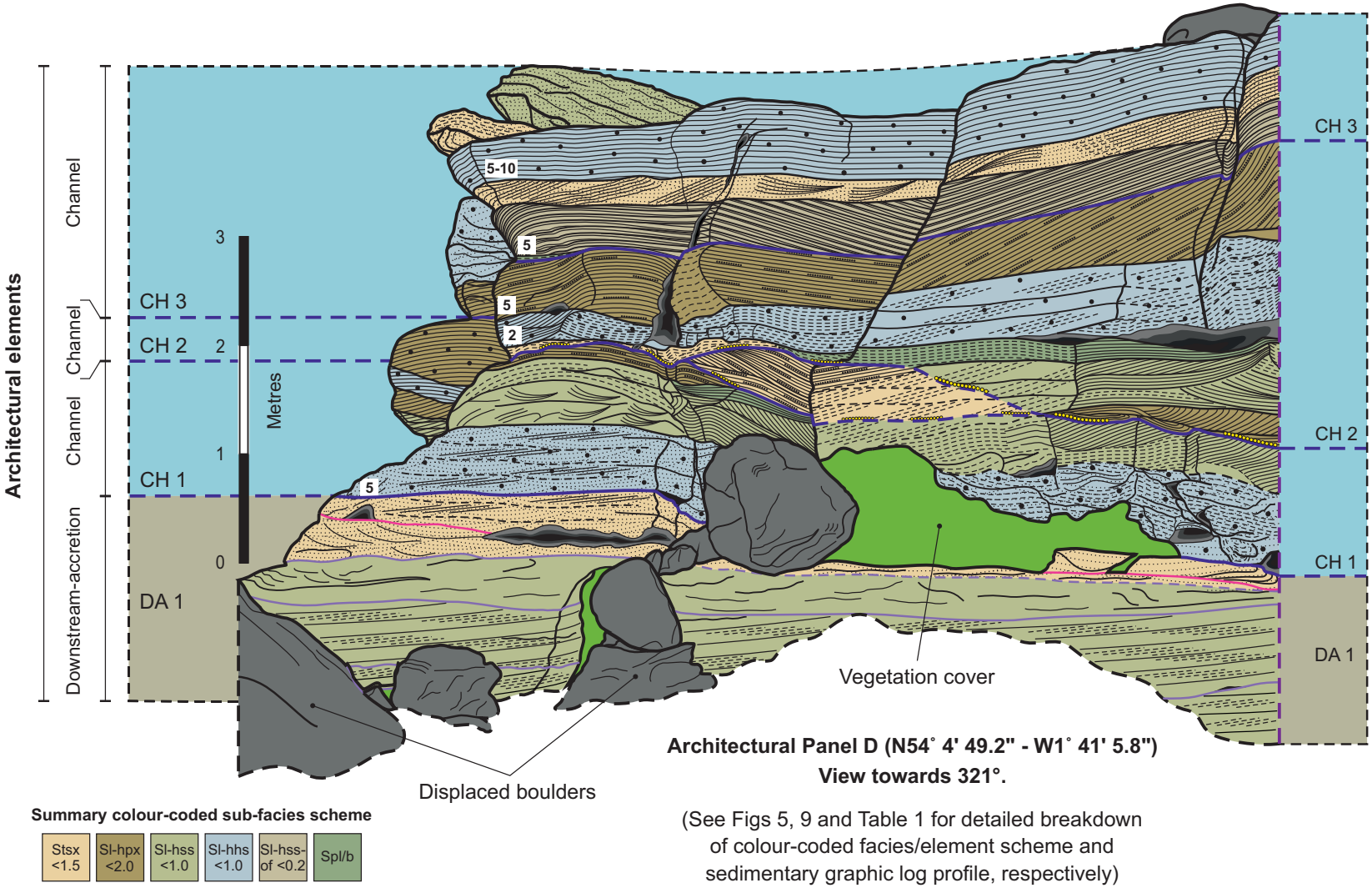


**Architectural Panel D (N54˚ 4' 49.2" - W1˚ 41' 5.8")**
**View towards 321°.**

(See Figs 5, 9 and Table 1 for detailed breakdown of colour-coded facies/element scheme and sedimentary graphic log profile, respectively)

**Fig. 8 Continued**

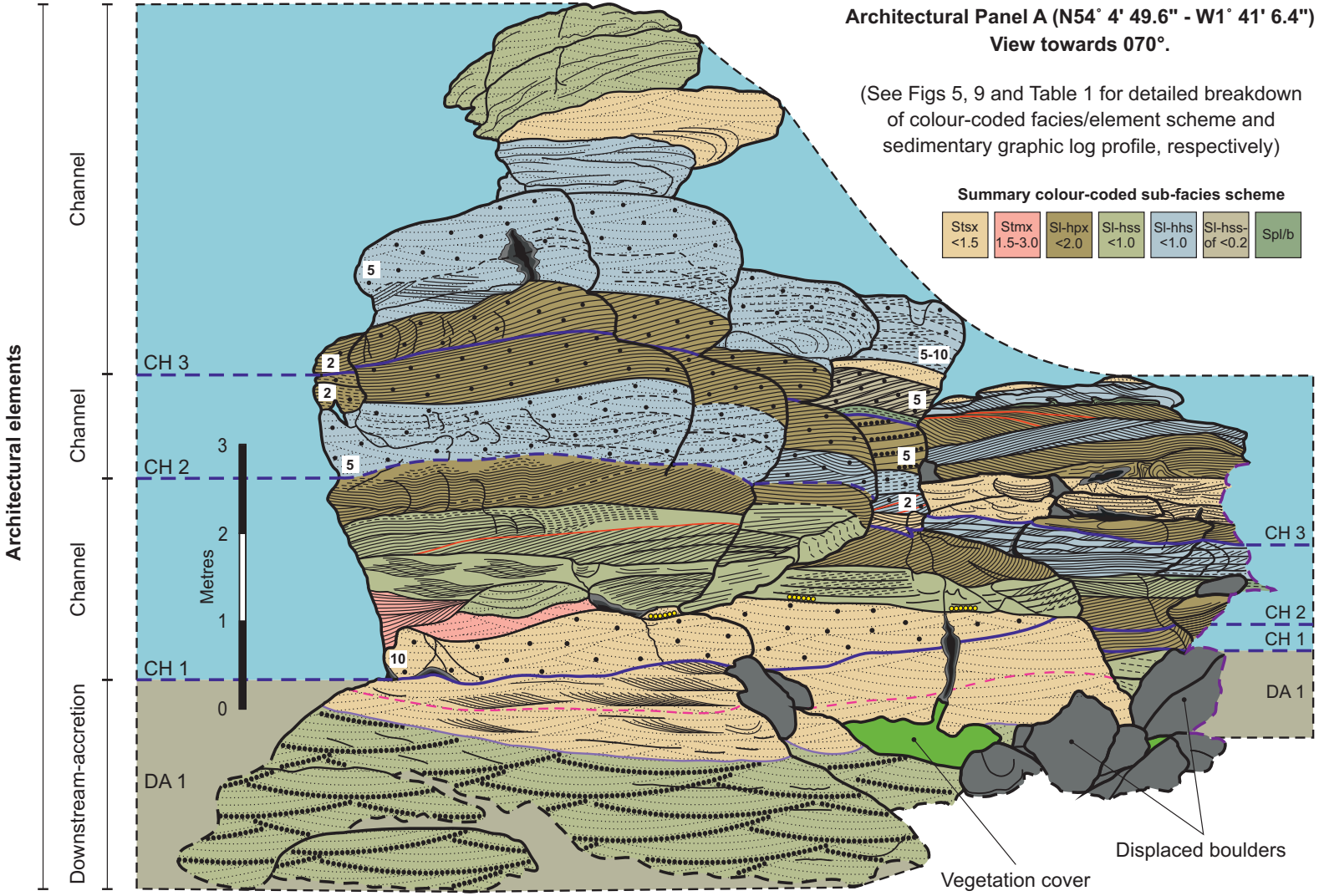


**Fig. 8**

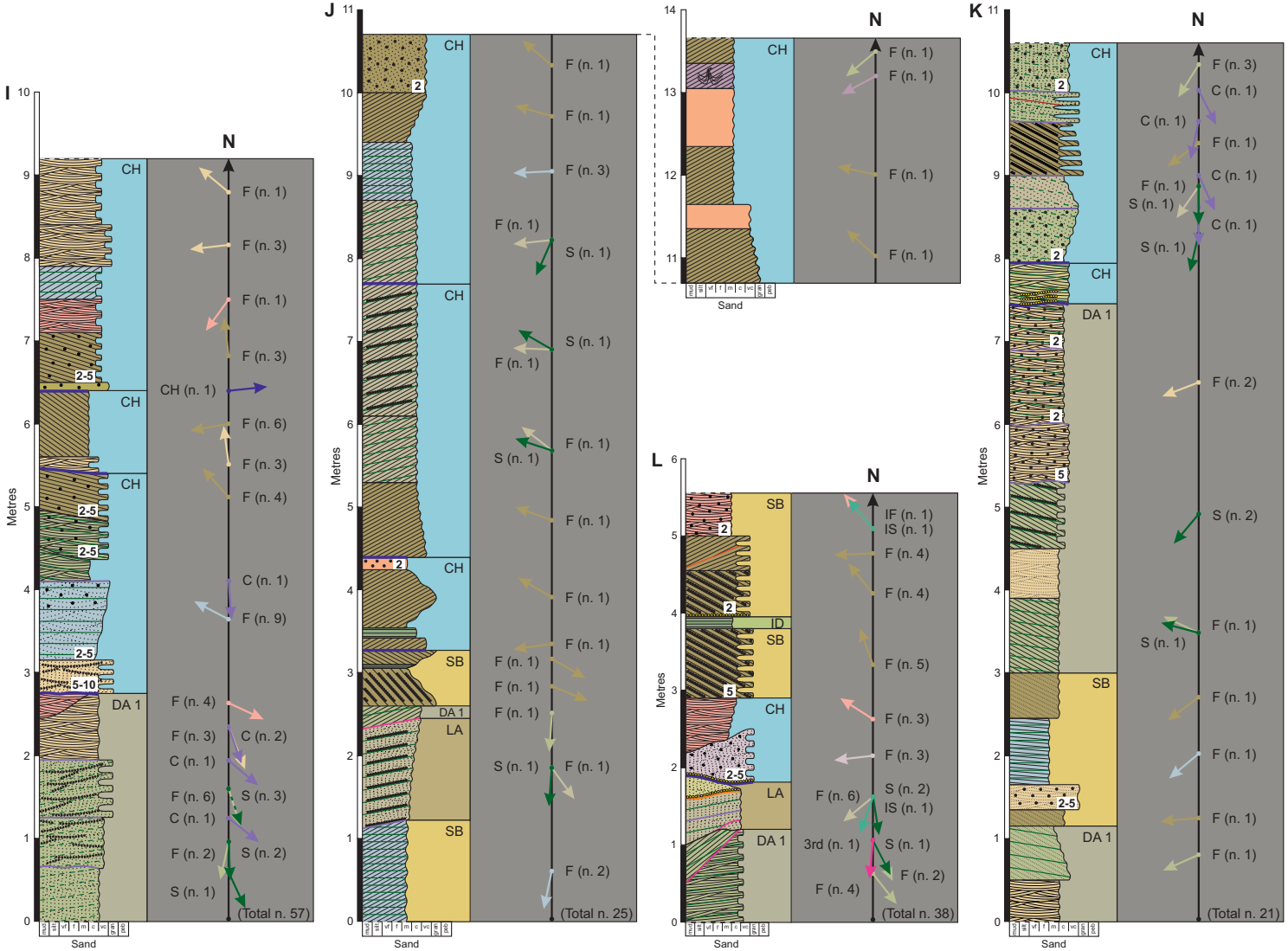


**Fig. 9 Continued**

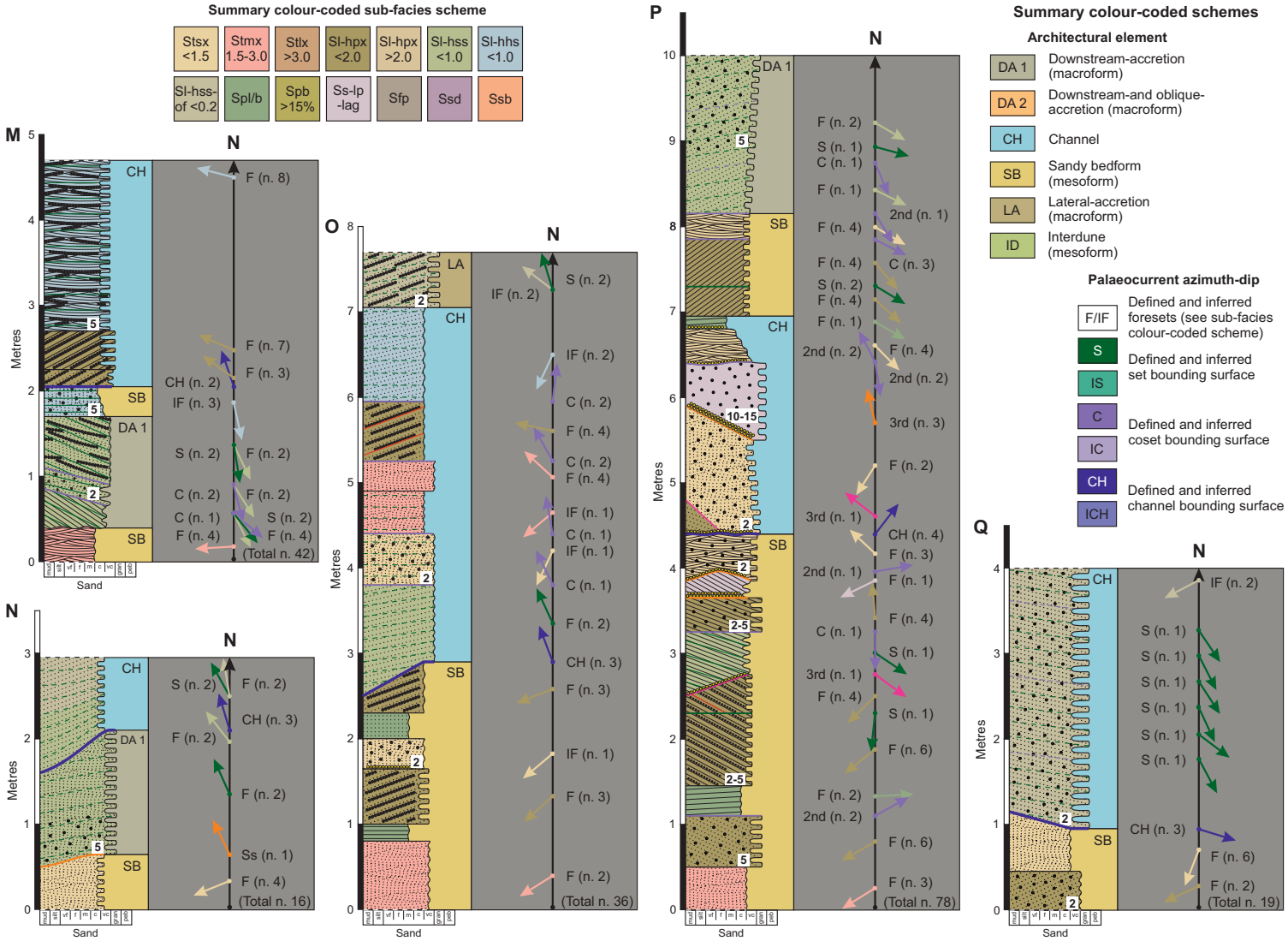


**Fig. 9 Continued**

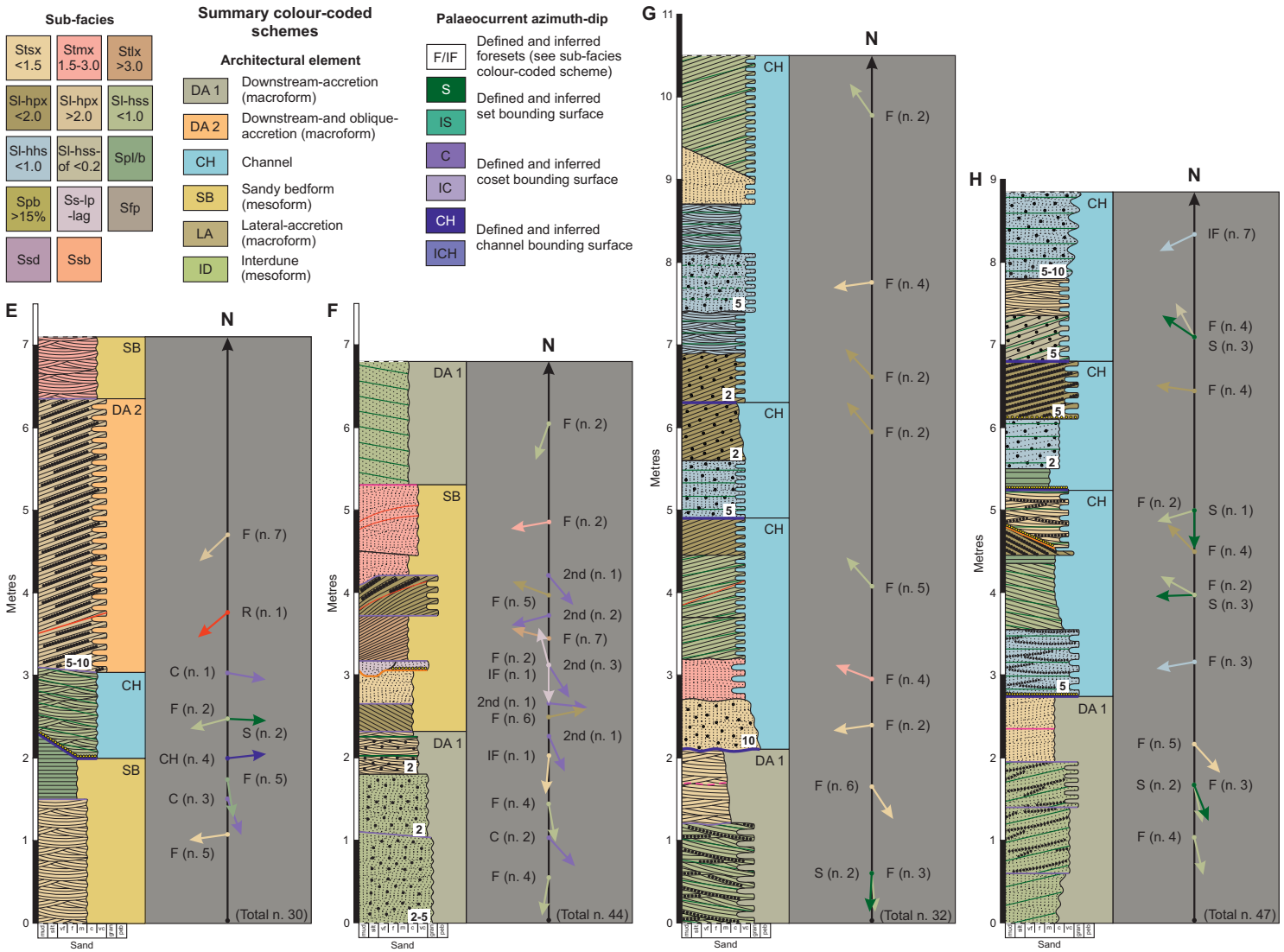


**Fig. 9**

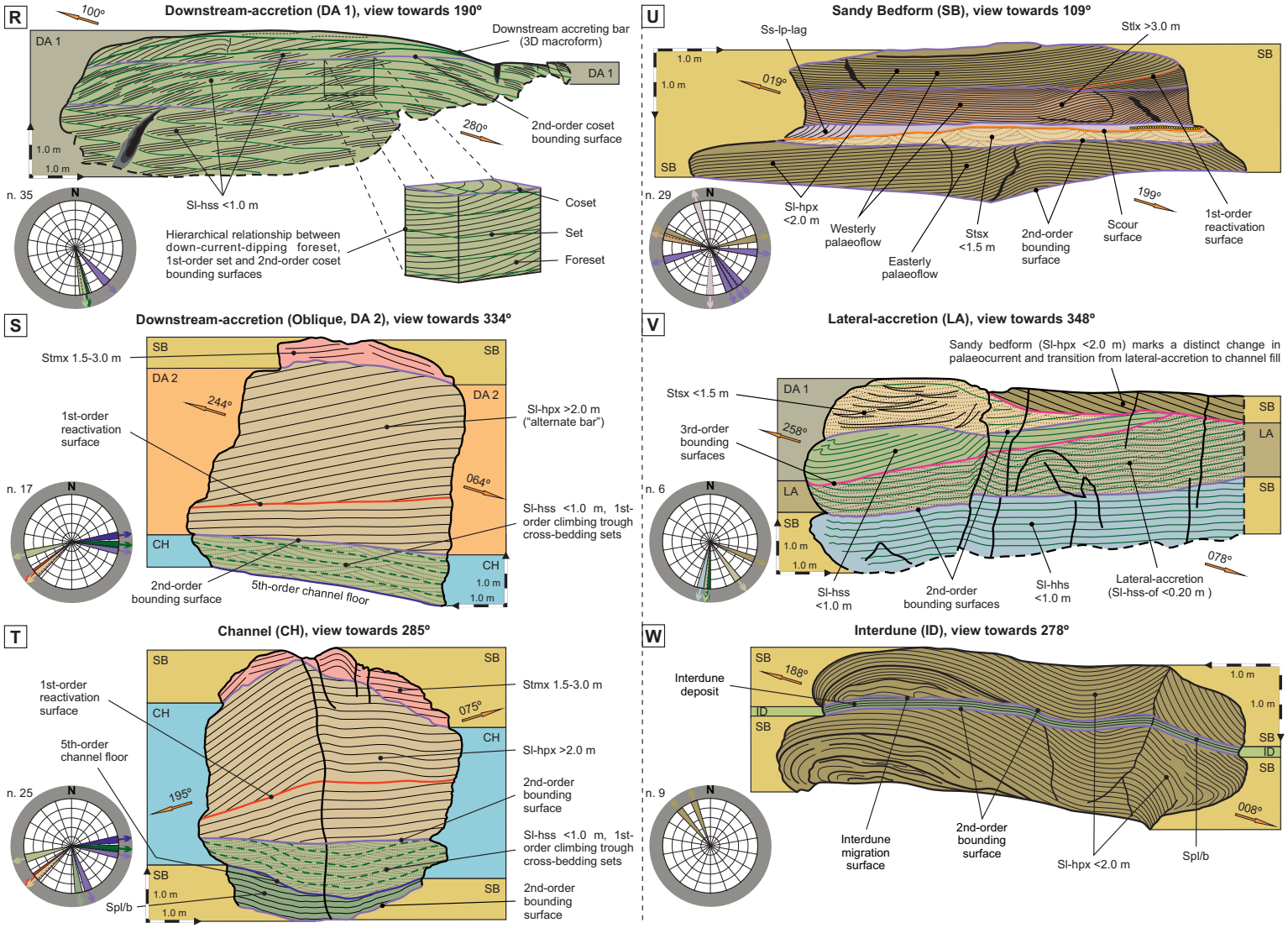


**Fig. 10**

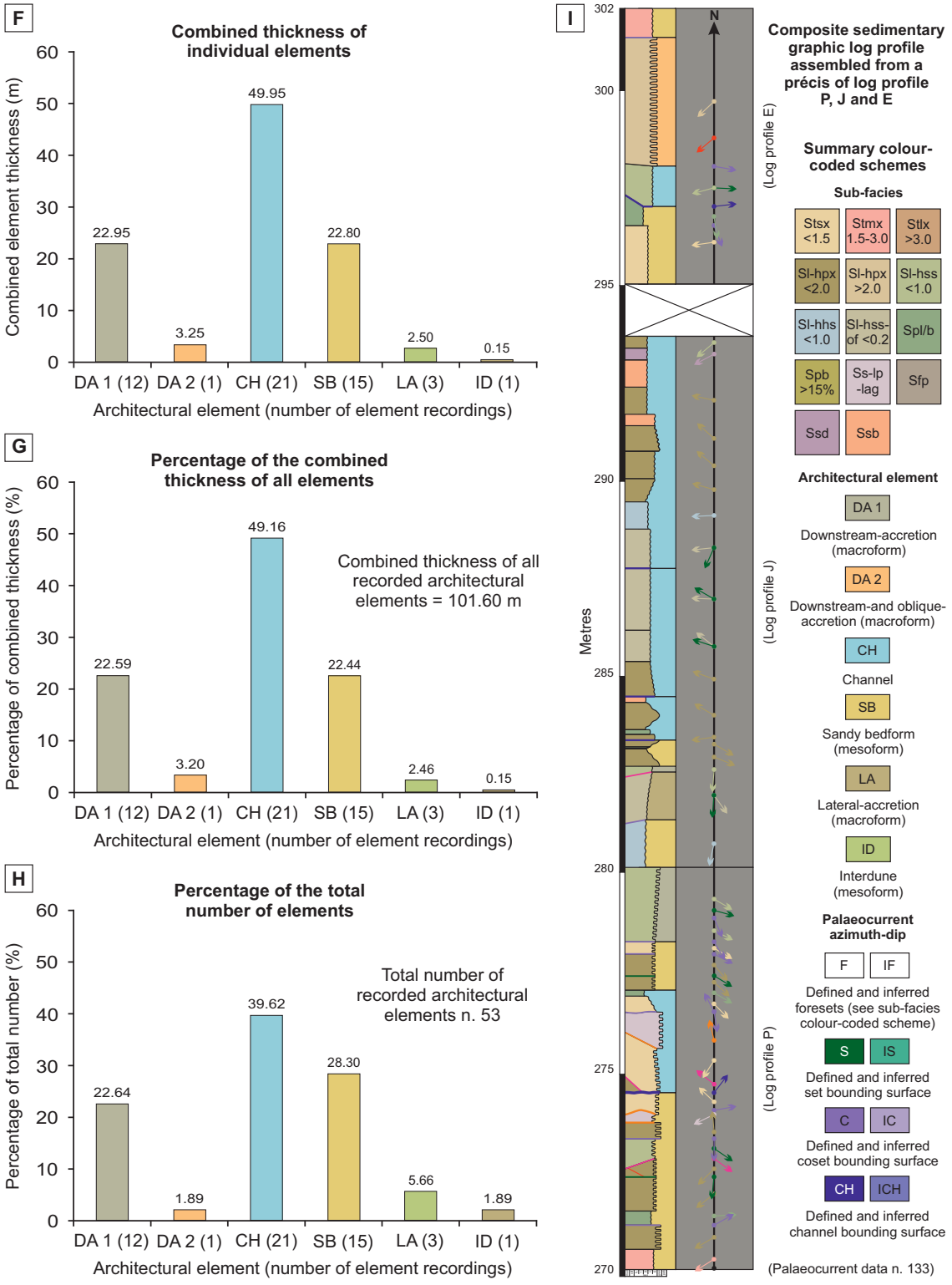


**Fig. 11 Continued**

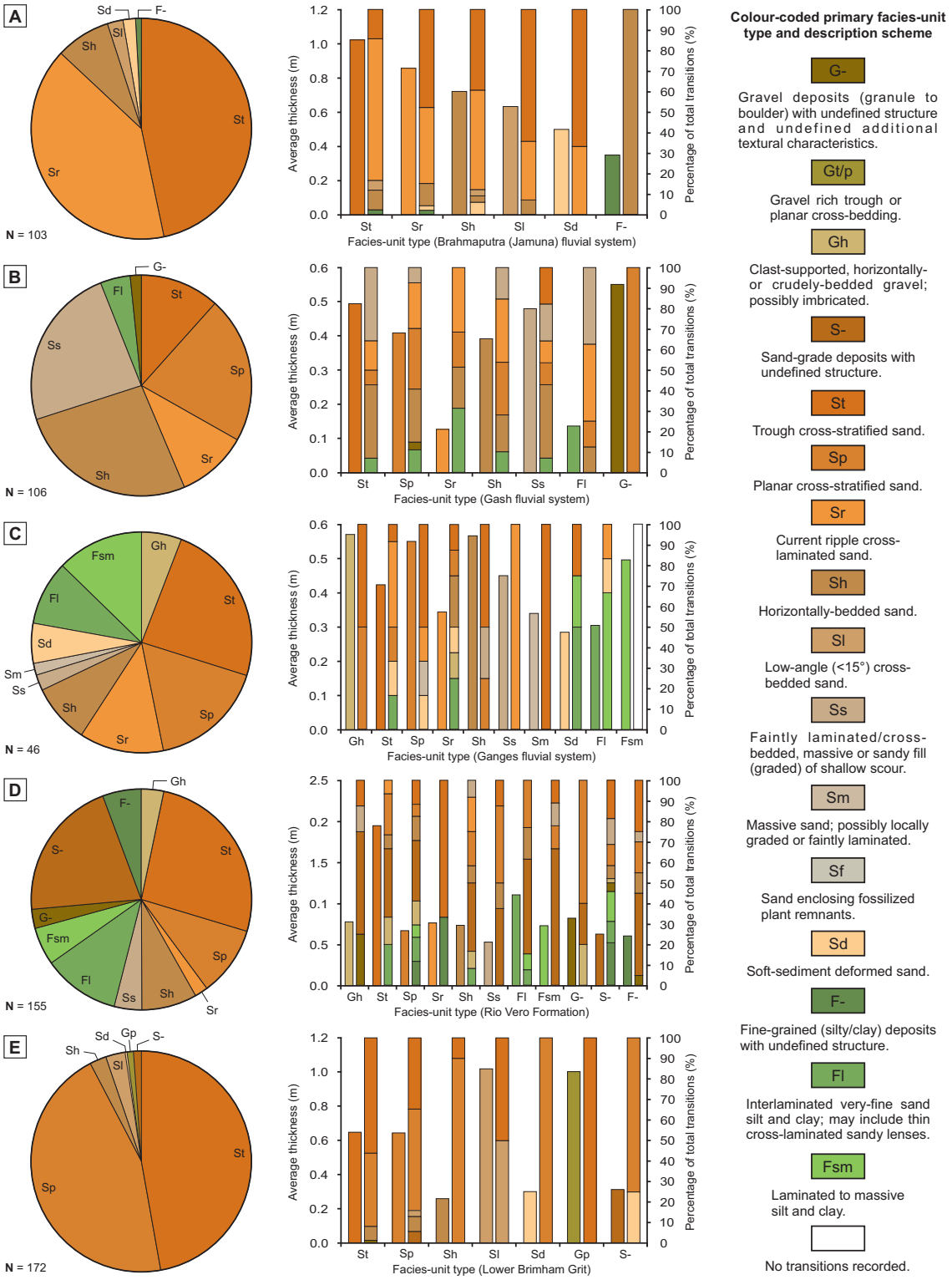


**Fig. 11**

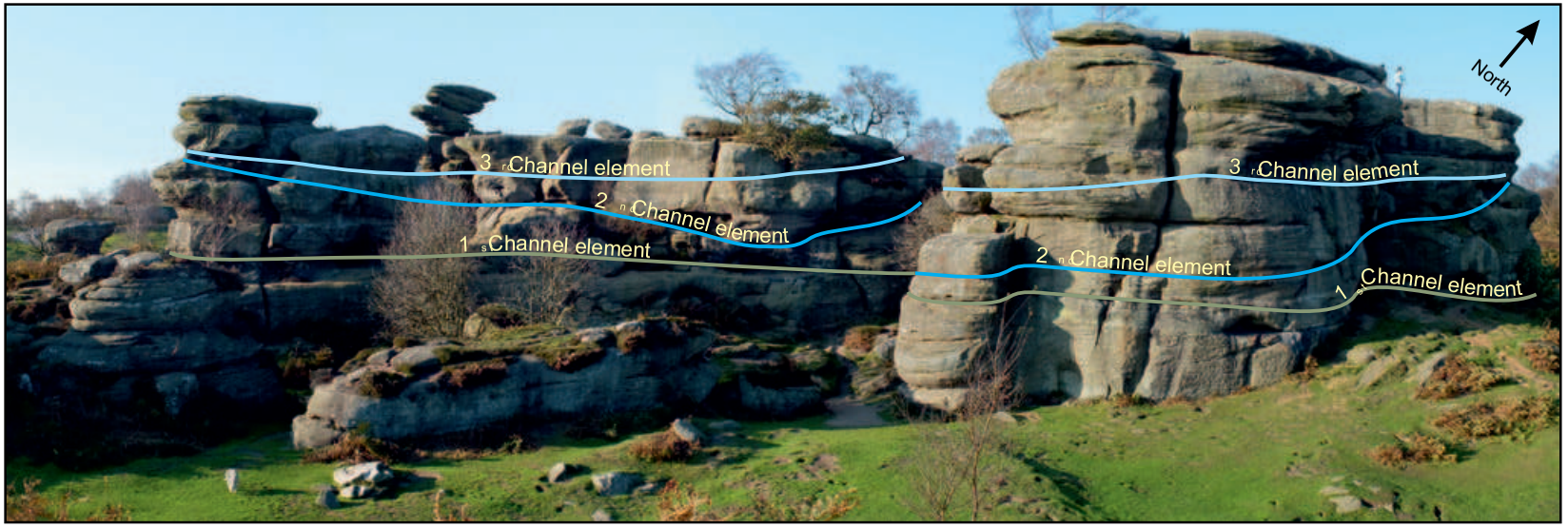


**Fig. 12**

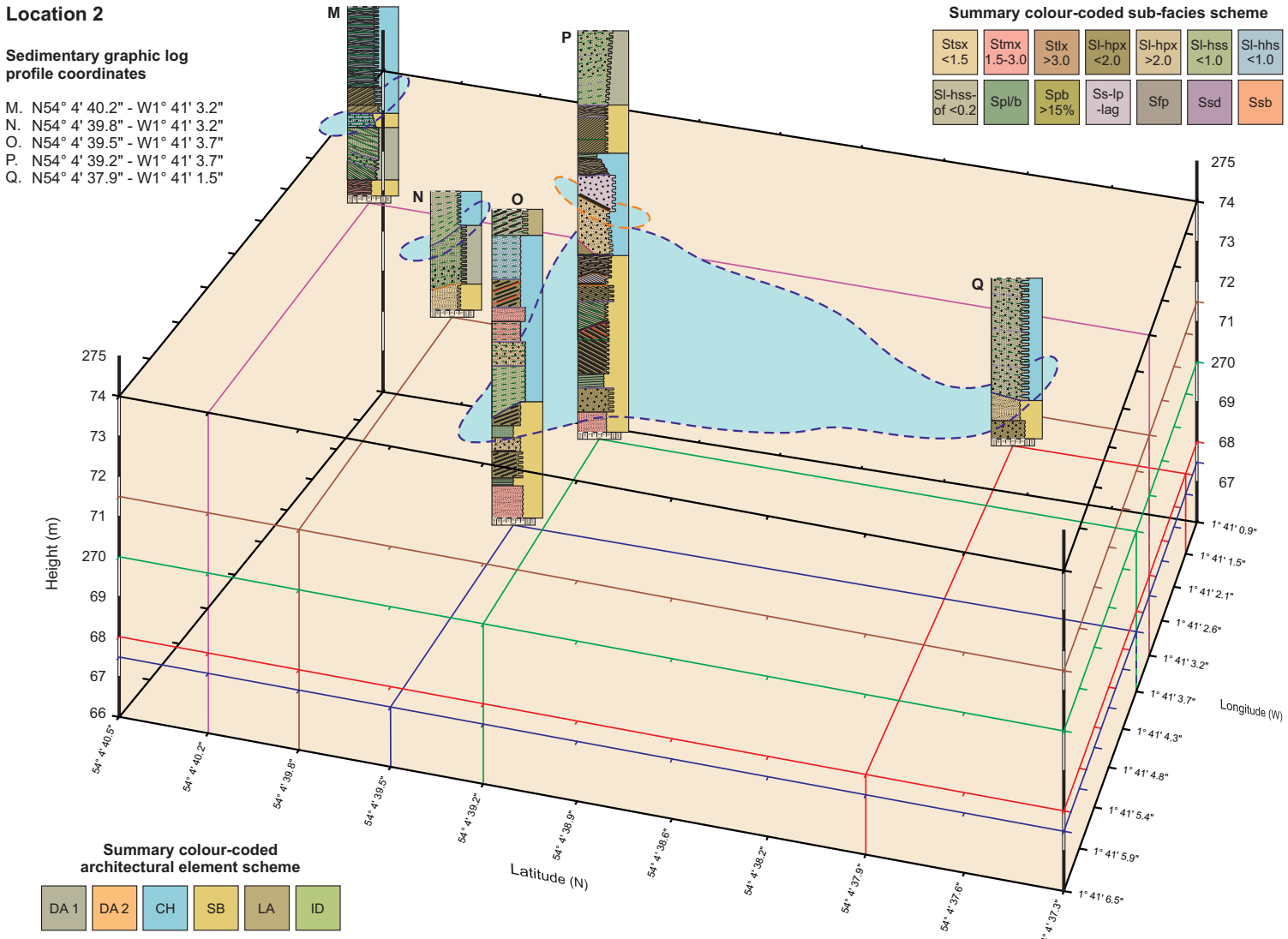


**Fig. 13 Continued**

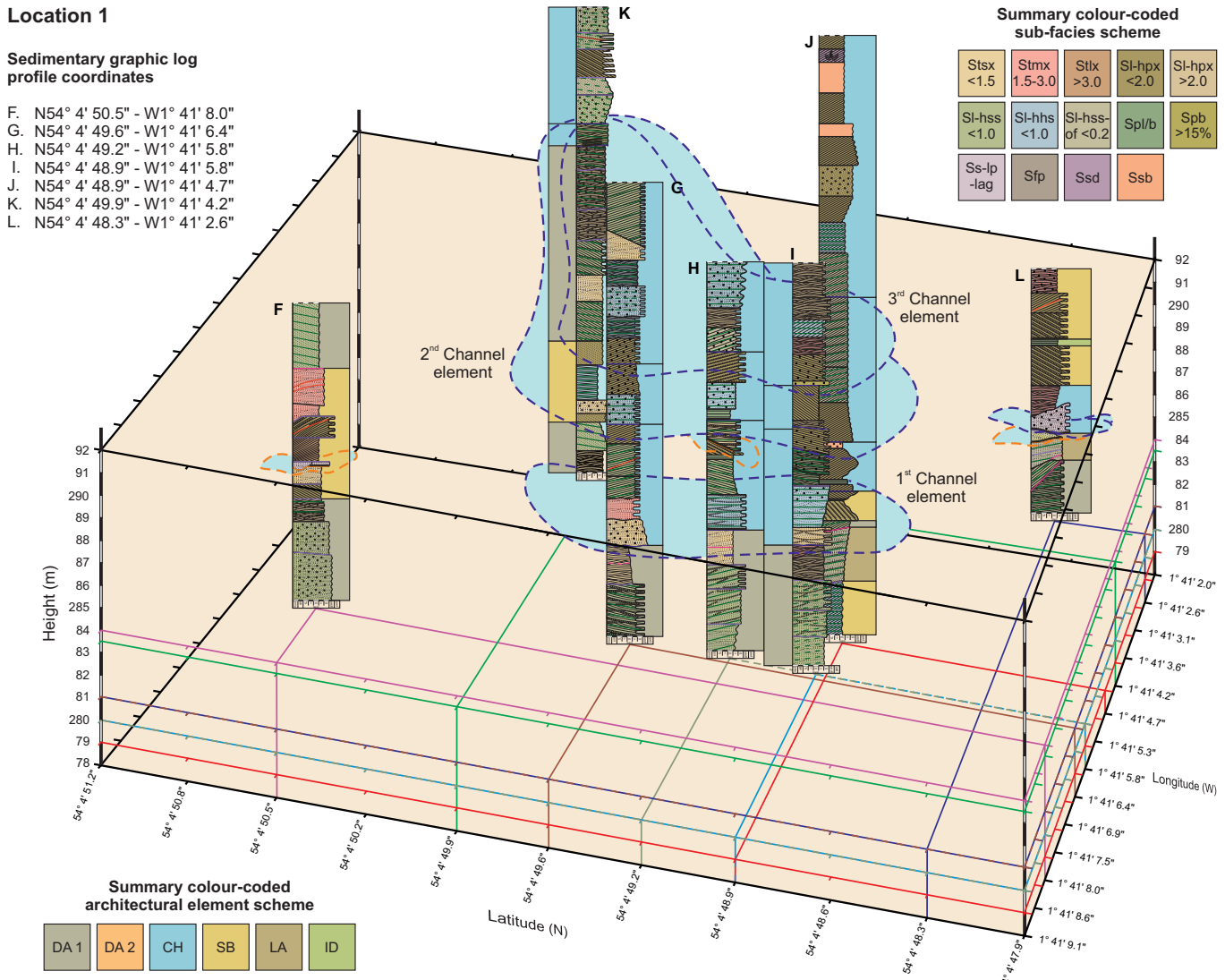


**Fig. 13**

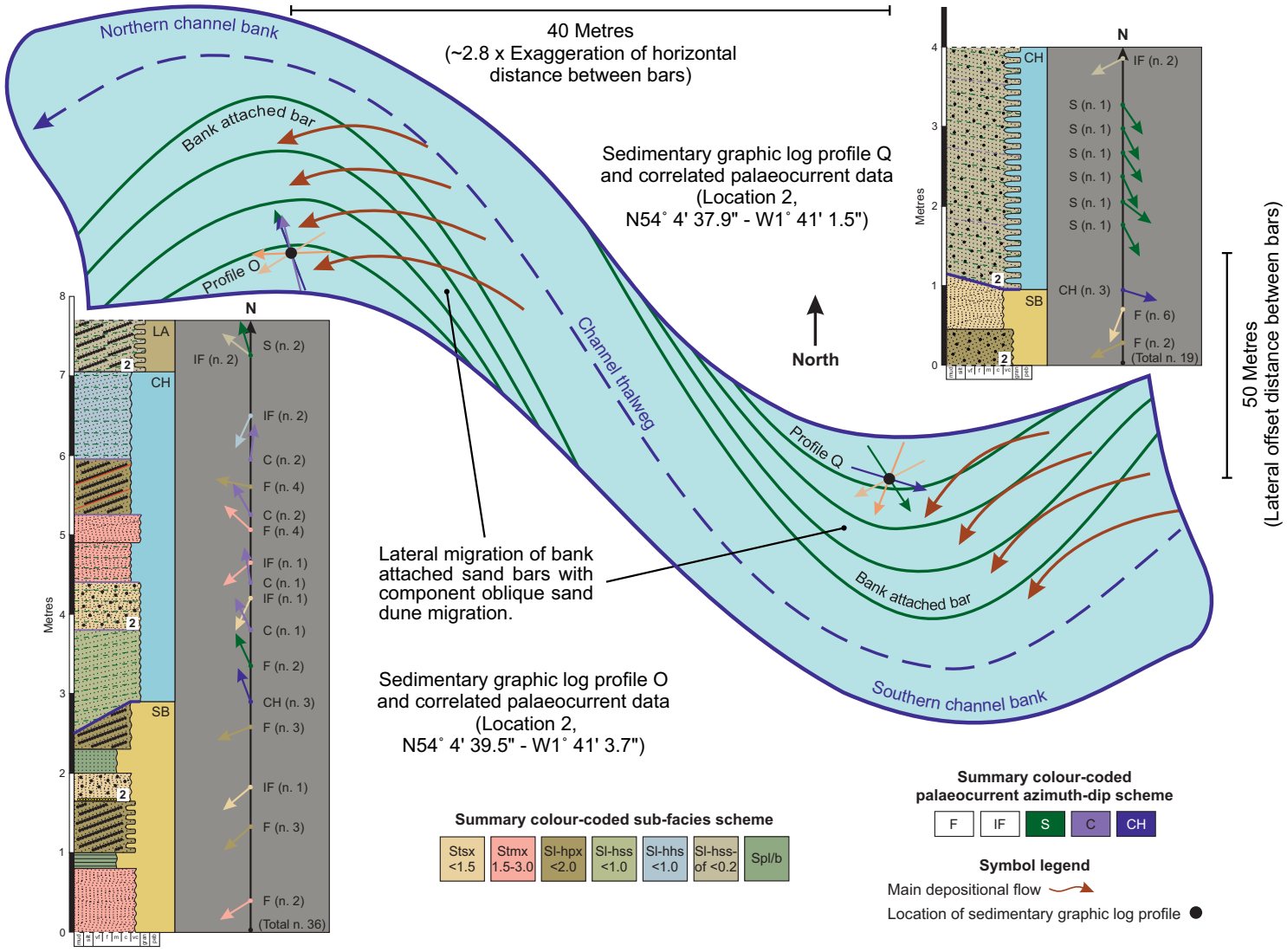


**Fig. 14**

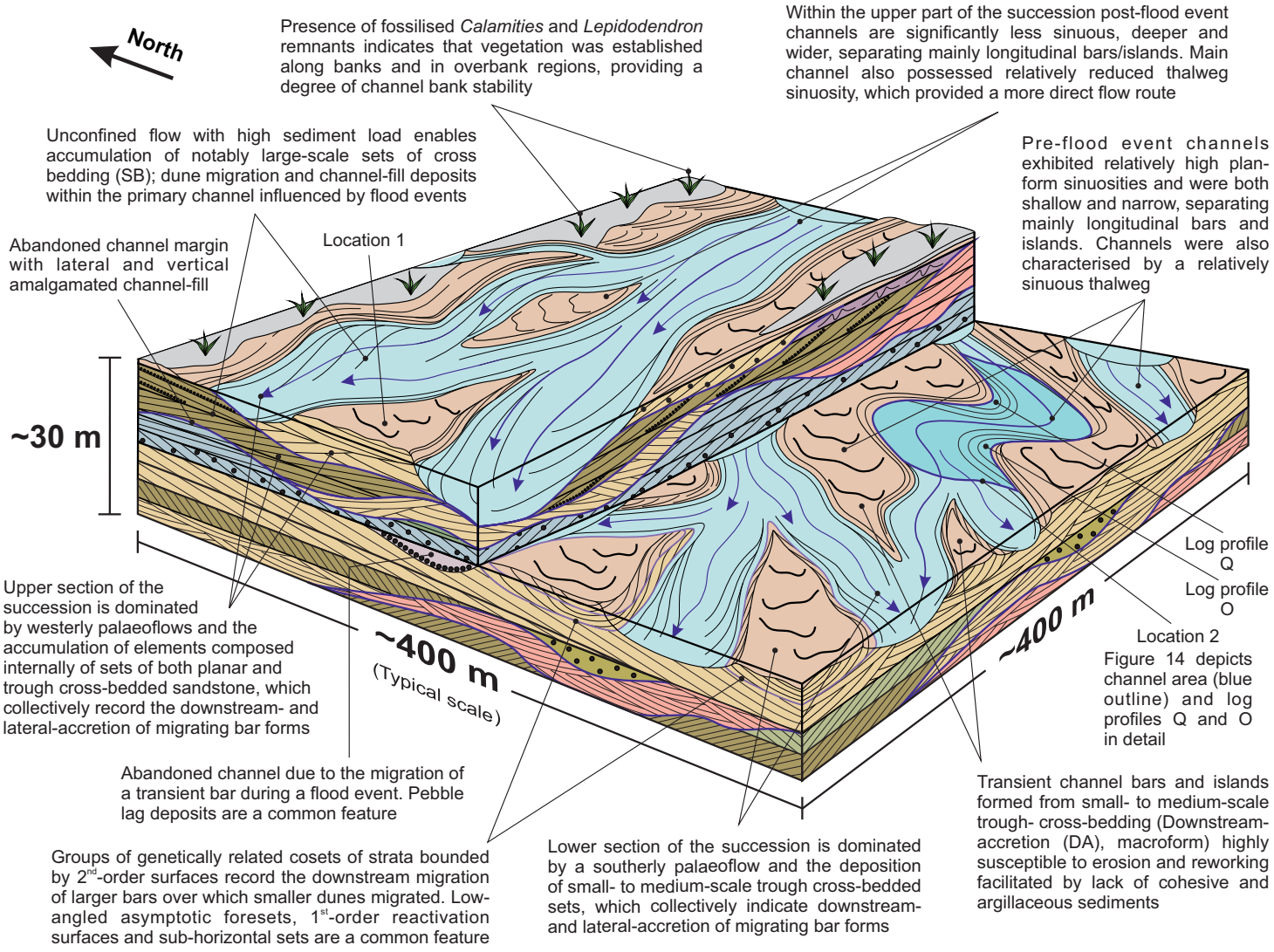


**Fig. 15**